Department of Civil Engineering
The University of Michigan

CYCLIC RESPONSE OF REINFORCED CONCRETE CONNECTIONS USING CAST-IN-PLACE SIFCON MATRIX

By
Hossam M. Abdou, Antoine E. Naaman
and
James K. Wight

ıry 1989 Report No. UMCE 89-1

A Report on a research Project Sponsored by
The National Science Foundation Grants
ECE-86-09579
and
ECE-86-15419

Ann Arbor, Michigan

ABSTRACT

The use of precast concrete in areas of high seismicity depends primarily on the development of a strong, ductile, and good energy dissipating connector between precast elements. The objective of this ongoing research is to develop such a connector for precast or precast prestressed concrete beam-column subassemblages. To acomplish this objective, twelve beam assemblages were constructed. The assemblages consisted of two precast concrete elements connected together to form a beam with a cast-in-place (CIP) joint using SIFCON as the matrix in the joint. Different steel arrangements were tried aiming at developing a hinging zone inside the CIP joint. The primary variables were the steel arrangements inside the CIP joint and the presence or absence of crack intiators at the top and bottom faces of the specimens.

There were four flexural failure locations: 1) outside the CIP joint, 2) the interface between the CIP joint and the precast segments, 3) inside the CIP joint with the steel yielding at the interface, and 4) inside the CIP joint with no steel yielding at the interfaces.

The primary objective of this study was reached for two of the combinations of variables when the flexural plastic hinge formed inside the CIP joint while the moment capacity at the interface was maintained at a desirable level.

ACKNOWLEDGMENTS

This investigation was supported by the National Science Foundation Grants No. ECE-86-09579 and No. ECE-86-15419 to the University of Michigan with Dr. S.C. Liu as NSF program director. The authors are very grateful for that support. Any opinions, findings, and conclusions erpressed in this paper are those of the authors and do not necessarily reflect the views of the sponsor.

TABLE OF CONTENTS

Page

ACKNOWLEDGMENTS ii

LIST OF TABLES v

LIST OF FIGURES vi

CHAPTER

I INTRODUCTION 1

1.1 General 1

1.2 Objective and Scope 2

1.3 Review of Previous Research 3

1.3.1 Precast Concrete 3

1.3.2 Fiber Concrete 5

II EXPERIMENTAL PROGRAM 8

2.1 General 8

2.2 Material Properties 9

2.3 Fabrication of Specimens 10

2.4 Test Setup 11

2.5 Loading Sequence 11

III TEST RESULTS 13

3.1 General 13

3.2 Crack Development and Failure Modes 13

3.3 Load vs. Displacement 13

3.4 Individual Specimen Behavior 14

IV EVALUATION OF TEST RESULTS 27

4.1 Comparison of the Theoretical and Experimental Results 27

4.2 Evaluation of Test Results 29

V SUMMARY AND CONCLUSION 32

4.1 Summary of the Test Results 32

4.2 Conclusion 33

4.3 Needed research 34

REFERENCES 36

LIST OF TABLES

TABLE Page

2.1 Parametric Details 43

2.2 Reinforcement Details 44

2.3 SIFCON Trial Mixes 45

2.4 Material Properties 46

3.1 Displacement Ductilities 47

4.1 Calculated and Actual Yield and Maximum Moment Outside the CIP Joint 48

4.2 Calculated and Actual Yield and Maximum Moments Inside the CIP Joint 49

4.3 Energy Dissipation of the Specimens 50

4.4 Cyclic Load Carrying Capacity of the Specimens 51

4.5 Shear Forces 52

4.6 Overall Performance 53

LIST OF FIGURES

FIGURE Page

2.1 Reinforcement Configuration in CIP Connections Tested with Beam Type Specimens 54

2.2 Stress-Strain Curves For SIFCON Trial Mixes under Compression Loading 55

2.3 Typical Stress-Strain Response of a SIFCON Mix..... 56

2.4 Stress-strain Model of the SIFCON Material under Compression..... 57

2.5 Stress-strain Model of the SIFCON Material under tension 57

2.6(a) The Assembly of the Precast Elements 58

2.6(b) The Placing of Fibers and the SIFCON Joint after Pouring the Slurry..... 59

2.7 Beam Type Configuration and Testing Set-up 60

2.8 Displacement Control Loading Sequence..... 61

3.1 Steel Configuration inside the CIP joint for Different Specimens 62

3.2(a) Load vs. Deflection Hysteresis Curve For Specimen B1 66

3.2(b) Load vs. Deflection Hysteresis Curve For Specimen B2 67
3.2(c) Load vs. Deflection Hysteresis Curve For Specimen B3 68
3.2(d) Load vs. Deflection Hysteresis Curve For Specimen B4 69
3.2(e) Load vs. Deflection Hysteresis Curve For Specimen B5 70
3.2(f) Load vs. Deflection Hysteresis Curve For Specimen B6 71
3.2(g) Load vs. Deflection Hysteresis Curve For Specimen B7 72
3.2(h) Load vs. Deflection Hysteresis Curve For Specimen B8 73
3.2(i) Load vs. Deflection Hysteresis Curve For Specimen B9 74
3.2(j) Load vs. Deflection Hysteresis Curve For Specimen B10 75
3.2(k) Load vs. Deflection Hysteresis Curve For Specimen B11 76
3.2(l) Load vs. Deflection Hysteresis Curve For Specimen B12 77
3.3(a) Specimen B1 at the End of the Test 78
3.3(b) Specimen B2 at the End of the Test 79
3.3(c) Specimen B3 at Failure 79
3.3(d) Specimen B4 at the End of the Test 80
3.3(e) Specimen B5 at Failure 80

3.3(f) Specimen B6 at the End of the Test 81

3.3(g) Specimen B7 at Failure 81

3.3(h) Specimen B8 at the End of the Test 82

3.3(i)Specimen B9 at Failure 82

3.3(j)Specimen B10 at the End of the Test..... 83

3.3(k)Specimen B11 at Failure..... 83

3.3(l)Specimen B12 at Failure..... 84

I. INTRODUCTION

1.1 General

It is true today that the design of connections in highly seismic zones is the foremost problem confronting the precast concrete industry. Increased efforts are being devoted presently to the connection problem in general, yet very few investigation have dealt with the ductility of connections for precast prestressed concrete structures. This research project is aimed at developing a new design technique for precast prestressed structures where precast elements will be jointed together away from the column face. The design will be such that the plastic hinge will form in the connector, where SIFCON will be used as the matrix material for this connector. SIFCON is a material which exhibits large ductility and has significant energy dissipation capacity.

This study is a part of an investigation at the University of Michigan aimed at developing a new earthquake resistant design and construction technique for structures made out of precast prestressed concrete members. Several new ideas are included in this research. These include:

Using a beam-column subassemblage made of precast reinforced or prestressed columns with short beam extensions,

connected to precast prestressed or partially prestressed beams.

Using a cast-in-place (CIP) joint, designed to serve as an energy absorbing plastic hinge, placed one beam depth away from the column face.

Using Slurry Infiltrated Fiber Concrete (SIFCON) as the primary matrix in the CIP joint to ensure high ductility, increase energy absorption, reduce spalling, and improve shear resistance during load reversals.

1.2 Objective and Scope

The main objective of the experimental part is to develop a strong and ductile cast-in-place joint (energy dissipating connector) between the precast column and the beam elements. As mentioned earlier, SIFCON will be used in this investigation as the matrix in the connector. In attempting to reach this objective, the following problems need to be addressed:

The inevitability of cracks at the interface between the cast-in place SIFCON and the precast elements. The opening of these cracks should be controlled to force the development of cracks inside the CIP joint.

The provision for an appropriate configuration of the reinforcement inside the CIP joint to ensure the desired ratio between the moment capacities of the sections at the CIP joint and the column face, as well as the development of the moment capacity of the concrete section at the interface.

The lack of information about SIFCON to be used as the joint matrix. Although SIFCON has been thoroughly investigated recently, such investigations have primarily been in the area of material testing. Less basic properties, such as the SIFCON rupture modulus, as well as the development length of the reinforcement steel in SIFCON, are yet to be better understood. Such an understanding could only stem from extensive testing of structural members where the effect of various parameters such as fiber length and diameter, as well as the mix properties are incorporated.

1.3 Review of Previous Research

1.3.1 Precast Concrete

Increasing attention has been devoted recently to the use of precast concrete elements in seismic areas[3,47] due mainly to the lack of provisions proper to the design of precast concrete in seismic areas. The design provisions developed for cast-in-place concrete structures should then be used for the design of precast structures. An overview of two seminars on the design of precast concrete for earthquake loading, as well as the suggested connection details for precast elements given in these seminars, are discussed in references[19,18,21]. The lack of a strong, ductile connector for the precast elements that possesses high energy absorption capacity is the major reason behind the reluctance to use precast construction in highly seismic areas. Such a connector, necessary for the development of a code provisions, has yet to be established.

Aiming at developing such a connection, Dolan et al.[16] tested beam-column connections made out of precast elements assembled together. Various methods of assemblages were used, such as field welding, bolting, post-tensioning, and connecting precast beams to cast-in-place columns. The authors stated that a low energy dissipation was noticed in all specimens, except the one having the cast-in-place column, and that better detailing could improve the behavior. However, the limited test data available from this study would prohibit drawing any conclusions about the performance of the connections suggested.

In another study by Clough,[11] the author developed a rational methodology for the derivation of the performance requirements of connectors for precast elements. This methodology stemmed from the design approach adopted by the Uniform Building Code,[46] and the Applied Technology Council.[3] Furthermore, the author illustrated this methodology by application to a seven story frame/shear wall parking structure. Conceptual drawings of appropriate connection details, which will be tested in a future phase, were proposed.

Bull and Park[32] studied the seismic resistance of frames incorporating precast prestressed concrete shells. The construction of these frames involves the use of U-shape precast prestressed shells as permanent formwork for beams. The core of the beams are then cast-in-place monolithically with the columns. Three exterior beam-column connections using this methodology of construction were tested. Two of these units were designed and detailed using the New Zealand Code[12] provisions for seismic loading. The interior surfaces of the U-shape precast beams were roughened before pouring the core concrete. However, one of the specimens was deliberately

debonded at the interface between the precast element and the cast-in-place concrete, in the region of the plastic hinge, in an attempt to improve the behavior. The authors stated that the behavior of the specimens was good and that they exhibited satisfactory strength and ductility. Moreover, the hysteresis loops were not pinched and indicated good energy dissipation capacity. The investigators also noticed that the deliberate debonding at the hinging region increased the length of the plastic hinge and prevented damage from occurring in the precast U-beam. The authors suggested that debonding should be used if damage in the precast U-beams is to be avoided during seismic loading.

1.3.2 Fiber Concrete

The addition of fibers to concrete leads to improvements in many of its mechanical properties such as flexure, tensile, and shear strength.[2,4,13,15,26] The most significant improvement imparted by fibers to a concrete matrix, which is particularly important for earthquake design, is the substantial increase in toughness or energy absorbing capacity. Higher improvements are expected from slurry infiltrated fiber concrete (SIFCON).

In conventional fiber concrete the fibers are premixed with the concrete matrix. In SIFCON, which is a relatively new material, the fibers are pre-placed in a mold so as to fill it completely and then infiltrated by cement slurry. Controlled by workability problems, fiber content in conventional fiber concrete is limited to 3% by volume, while 20% can be attained in SIFCON depending on the geometric properties of the fiber used. In SIFCON the fiber content and the fiber geometric properties influence the

void size between the fibers and thus the fineness of the slurry used. Compressive strength of up to 20 ksi and strains of up to 10% have been reported for SIFCON specimens.[23] The strength and toughness characteristic of SIFCON have already been exploited in several applications such as impact resistant structures and industrial floors.[27] However, no studies have investigated the use of SIFCON for seismic applications.

Few research studies dealt with fiber concrete under load reversals. Jindal and Hassan[25] tested six beams with short column stubs, four of which were made out of Fiber Reinforced Concrete (FRC). They reported a significant increase in shear capacity and ductility with the addition of fibers. Henager[22] tested beam-column connections using steel fibrous concrete in the column region. The results of these tests indicated that the utilization of fibers increased the stiffness and ductility of the assemblage, and provided good confinement in the joint region which subsequently demanded less hoop reinforcement in the connection. Nishioka et al.[31] tested cantilever beams, using fibrous concrete, under repeated loading. They found out that the specimens with fiber concrete showed better resistance to shear deterioration by preventing slippage. Craig et al.[14] tested exterior beam-column connections with different shear span to depth ratios to explore the use of conventional fiber concrete in seismic applications. They used fiber reinforced concrete (1.5% by volume) in the joint region in a monolithically cast beam-column assembly to improve the seismic response of the joint. They found out that the addition of fibers in the joint region provided better confinement of the concrete, showed less structural damage, and maintained the integrity of the joint better than normal concrete.

A significant increase of energy dissipation, higher resistance to bond deterioration, and increase in the shear capacity were also reported.

Balaguru and Ezeldin[5] tested partially prestressed concrete beams using high strength fiber concrete with various fiber content ranging between 0-1.5% by volume. The specimens were designed to fail in shear. The shear span to depth ratio was kept at 2.6 for all specimens to evaluate the contribution of fibers to shear resistance. They concluded that addition of steel fibers resulted in an increase in the cracking moment and a reduction in crack width and crack spacing. Moreover, they also reported that for low shear spans the contribution of fibers to shear strength was not significant.

Sood and Gupta[41] in an experimental investigation to study the behavior of beam-column connections reported that the use of fiber concrete increased the cracking strength by a factor of 2, retarded crack growth and reduced crack width by as much as 25% when compared to conventional concrete joints. They also stated that the post cracking rotational capacity of fibrous joints at failure can be 3.6 times that of the corresponding conventional joints. Due to the improved shear behavior of fibrous joints, they suggested the elimination of joint shear reinforcement to reduce the congestion of reinforcement in this region. Jindal and Sharma[24] also tested knee-type fibrous beam-column connections and concluded that the use of fibers is effective in increasing ductility and crack resistance in the connection region. They reported that the ultimate rotation of fibrous connections was 6 to 9 times that of the conventional reinforced concrete connections.

II. EXPERIMENTAL PROGRAM

2.1 General

The experimental program described in this report consists primarily of twelve reinforced concrete beams with a Slurry Infiltrated Fiber Concrete (SIFCON) joint in the middle. These specimens were built from two precast reinforced concrete parts connected with a cast-in-place (CIP) joint filled with a SIFCON matrix. This stage of the program followed a preliminary investigation of two beam-column connection prepared to explore the idea of creating a plastic hinge in a SIFCON joint at a distance one beam depth away from the column face. Testing of beam-column type specimens was temporarily interrupted, however, due to the lack of information on some basic properties of SIFCON, and an appropriate reinforcement arrangement for forcing a plastic hinge to form in the CIP joint.

For the beams tested the compressive strength of SIFCON was kept lower than that of the precast elements because it was thought that the higher strength could be detrimental to the behavior. The parameters tested were the arrangement of the reinforcing steel inside the SIFCON joint and the presence or absence of crack intiators in the middle of the CIP joint. The various parameters investigated are listed in Table 2.1.

The primary objective of this program was to find an acceptable reinforcing steel configuration in the SIFCON joint so as to ensure the oc-

curence of a plastic hinge inside the CIP joint during cyclic loading. The lack of information about SIFCON as a matrix led to five trials of steel arrangements as shown in Fig. 2.1. Table 2.2 summarises the reinforcements and the corresponding steel arrangements for each specimen.

2.2 Material Properties

The beam specimens were designed to have a 28-day concrete strength of 6000 psi. Concrete for the specimens was obtained from a local ready mix plant. The concrete mix was designed using Type I Portland Cement and a graded gravel with one-half inch maximum aggregate size. The water to cement ratio was selected to produce a workable mix and facilitate compaction. From each batch a sufficient number of 4 in. x 8 in. cylinders were prepared to determine the concrete compressive strength at 28 days and at the time the specimens were tested.

For the CIP joint, an acceptable SIFCON material was found after numerous trial mixes. It consisted of:

> One part Type III cement, two parts fine ottawa sand (ASTM C-109), and 0.6 parts of water, all by weight.
>
> Hooked steel fibers 2 in. long, 0.02 in. in diameter and the fiber content was 4-5% by volume.

The details of the trial mixes and their respective stress-strain curves are given in Table 2.3 and Fig. 2.2 respectively.

Because it was important to improve shrinkage properties of the SIFCON material, sand was used in the mix to produce mortar slurry in-

stead of a cement slurry, as has commonly been used in SIFCON applications. To improve the penetration of the mortar slurry, longer fibers with a larger diameter were used to create acceptable voids in the fiber network. A typical stress-strain response to monotonic and cyclic compression loading of the SIFCON mix selected is shown in Fig. 2.3.

Unlike fiber concrete, SIFCON is a relatively new material and its mechanical properties are not yet well documented. Two assumption were used in calculating the moment capacities of sections using SIFCON. The first being the use of the model shown in Fig. 2.4 to charactarize the stress strain behavior of SIFCON in compression. This model was assumed to be the best representation for the low strength SIFCON that was being used. The second assumption was the model characterizing the stress-strain relationship of SIFCON in tension. This model, shown in Fig. 2.5, assumes that after cracking the tensile capacity for SIFCON will remain constant up to three times the cracking strain.

Grade 60 No. 3, and No. 4 bars were used for the main reinforcement in the beams. The beam stirrups were fabricated from 3/16 in. diameter khurled bars. Table 2.4 gives the material properties of the concrete, SIFCON, and steel used in this investigation.

2.3 Fabrication of Specimens

Each beam specimen consisted of two precast concrete elements connected together by the SIFCON material in the Cast-in-place (CIP) joint. The dimensions of all the beams were the same. The forms were sealed and their interior surfaces were oiled prior to casting to facilitate disassembly after hardening of the concrete.

Reinforcing cages were placed inside the oiled forms of the precast elements, with steel to be used inside the CIP joint protruding from one end. Concrete was then poured from a ready mix truck. A hand held vibrator was used to concolidate the concrete in the forms.

After hardening of the concrete for the precast elements, the forms were removed and the precast elements were put together where the protruding steel from both elements overlaped to form the joint. Wooden forms were put around the joint, steel fibers were placed to fill the joint and the selected mortar mix was used to infiltrate around the fibers and fill the joint. Figure 2.6 shows photographs of the different stages in assembling the precast elements with the SIFCON joint.

2.4 Test Setup

The specimens were tested in four point bending using a specially modified INSTRON servohydraulic testing machine (system 8000) with a 120 kip actuator. A steel spreader beam was attached to the load cell and loading pads were attached to the beam at the desired loading points. The specimens were put on two hinge supports; one was fixed and the other was able to move in the horizontal direction. A system of I beams and round steel bars were used to fabricate the supports and the loading pads in the upward direction. The testing set-up and specimen dimensions are shown in Fig. 2.7.

2.5 Loading Sequence

For all specimens the test was controlled by the displacement of the specimen at the points of load application according to the loading history

shown in Fig. 2.8. This loading schedule was found in previous studies to give sufficient information about the strength as well as stiffness loss of the specimen.

Lateral Displacements applied were controlled in terms of displacement ductilities. The displacement ductility was defined as the ratio of load point displacement at any stage during the test to the corresponding displacement at the initial yielding of the beam longitudinal reinforcement.

The displacement ductilities applied to the specimens were based on the actual yield displacement observed from the load-deflection curves. In the first cycle 75% of the calculated yield capacity was applied, followed by a cycle to determine the actual yield capacity of the specimen. Cycles to displacement ductilities of two, three, and four followed, depending on the capacity of the specimen.

III TEST RESULTS

3.1 General

The overall behavior of the test specimens will be discussed using two sources of informations:

1. Photographic record of each specimen.

2. The Total Actuator Load vs. Displacement under load points curves (Hysteresis Loops).

3.2 Crack Development and Failure Modes

Flexural cracks appeared in the beams, as well as at the interfaces of the CIP joint, as soon as the specimens were loaded. The two cracks at the interface of the concrete and the CIP joint continued to widen as the test progressed. Their width increase was a function of the reinforcing arrangement inside the CIP joint. Also the arrangement of steel inside the CIP joint affected the location of failure.

3.3 Load vs. Displacement

The load-displacement curves (hysteresis loops) are shown in Fig. 3.2(a) to 3.2(l). Due to set-up difficulties it was not possible to achieve an identical specimen behavior in the upward as well as the downward

direction although the specimens were symmetrical, top and bottom. This was primarily due to the deformations in the loading and the supporting elements in the upward direction. Also, it was not possible to satisfy the intended loading sequence for all the specimens. The achieved maximum displacement of each cycle relative to the yield cycle, referred to as the displacement ductility, is given in Table 3.1 for all specimens.

The level of load for each specimen indicated whether the plastic hinge formed outside or inside the CIP joint. The hysteresis loops also showed whether the cutoff bars experienced any slippage or not, and thus their ability to develop the moment capacity of the concrete section at the interface. The following is a discription of the particular behavior of each specimen.

3.4 Individual Specimen Behavior

Specimen B1

The arrangement of the steel inside the joint of this beam is shown in Fig. 3.1(a). This specimen was reinforced by 4 #4 top and bottom bars in the precast concrete elements. Two bars were bent at a 45° angle inside the CIP joint and were cutoff in the middle section of the CIP joint. The other two were looped and were extended the full length of the joint. In this specimen crack intiators (thin aluminum plates which penetrated 0.75 in. into the CIP joint) were put along the top and bottom faces of the beam in the middle of the CIP joint.

During the first cycle cracks formed in the shear span as well as at the joint interfaces. In the next cycle the cracks in the shear span ceased

to widen while those at the interfaces continued to widen. As the test progressed a crack formed parallel to the inclined bars inside the CIP joint and was connected to the crack developed by the crack intiator at the bottom of the beam. Ultimately, failure occurred at the interface for downward loading and in the CIP for upward loading. Figure 3.3(a), shows Specimen B1 in the downward loading direction during the test and at the end of the test in the upward loading direction.

From the load-deflection curve, Fig. 3.2(a), it can be observed that the specimen started to yield at a load producing 11 kips of shearing force in the beam (total load of 22 kips). This force is much smaller than the shear capacity expected if failure was to occur at the interface. This indicates that there was a significant slip of the cuttoff bars inside the CIP joint as indicated by the inclined cracks. Thus, the full moment capacity at the interface could not be developed and a premature failure occurred. A substantial loss in the load carrying capacity and stiffness with cycling, as well as severe pinching and low energy dissipation, marked the behavior of this specimen.

Specimen B2

Specimen B2 was reinforced with 4#4 top and bottom bars in the precast elements. Two of the bars were looped and were extended the full length of the CIP joint. The other two were extended straight to the end of the CIP joint. This was done to increase the anchorage length of the cutoff bars in an attempt to develop the full moment capacity at the interface locations. The arrangement of the steel for this specimen is shown in Fig. 3.1(b).

During the first cycle flexural cracks appeared in the shear span and at the interfaces. In the subsequent cycles one of the cracks at the interfaces started to pickup all the deformation with minor extra cracking outside the CIP joint. Throughout the test the CIP joint remained intact. The failure occurred at the interface when concrete in the precast elements started to crush. The specimen at the end of the test is shown in Fig.3.3(b).

As observed from the load-deflection curve, Fig. 3.2(b), the shear force sustained by this specimen was 15 kips. This was smaller than the expected capacity if failure was to occur outside the CIP joint. This implied that slip of the straight cutoff bars occurred during loading, thus preventing the development of the full moment capacity at the interface. The specimen was loaded through five cycles with a maximum displacement ductility of 3.5, and suffered a loss of 20% in its load carrynig capacity.

Specimen B3

Specimen B3 was reinforced with the same amount and with the same arrangement of steel as Specimen B2, Fig. 3.1(b). Crack intiators, however, were placed at the top and bottom faces of the beam in the middle of the CIP joint. This was done to help induce cracks inside the CIP joint since SIFCON has a high modulus of rupture. It was believed that the high modulus of rupture was the primary reason why no plastic deformation was introduced inside the CIP joint of Specimen B2.

Similar to Specimen B2, cracks occurred in the shear span and at the interfaces during the first cycle of loading. One of the cracks at the inter-

face began to widen as the test progressed. During testing, only minor cracking inside the CIP joint was visible, and was attributed mainly to the presence of crack intiators. Figure 3.3(c) shows the specimen at failure.

From the load-deflection curve, Fig. 3.2(c), the maximum shear force attained was 17.5 kips. Although this value was a little higher than that for Specimen B2, it was still insufficient to develop the full moment capacity at the interface where failure occurred. Thus, some slippage in the staight cutoff bars was probable. The specimen was loaded through five cycles, reaching a maximum displacement ductility of 3.7 with a 30% loss in load carrying capacity and a considerable reduction in stiffness.

Specimen B4

Specimen B4 was reinforced with 4#4 top and bottom bars in the precast concrete elements. All four bars were looped to provide continuity in the reinforcement. Two of the bars were extended 3" inside the CIP joint, the other two were extended the full length of the CIP joint, i.e. 10", Fig. 3.1(c). The cutoff bars were looped and horizontal steel rods were placed at the corners of the loop to improve the anchorage. This was believed to increase the anchorage of the cutoff bars which in turn would help in attaining the moment capacity of the sections at the interface locations.

After minor cracking in the shear span and at the interfaces during the first cycle, cracks started to occur in the CIP joint. These cracks did not start from the top fibers of the beam, but rather from within. Cracks inside the CIP were mainly around the cutoff bars. This indicated that

slippage of the cutoff bars might have occurred. Figure 3.3(d) shows the specimen at failure.

From the load-deflection curve, Fig.3.2-d, it can be concluded that the specimen performance was satisfactory at least during the first three cycles of loading. The specimen was loaded through four cycles with maximum displacement ductility of 3.5. A sudden drop of strength and stiffness and excessive pinching marked the behavior in the fourth cycle. Failure at one of the interfaces with a maximum shear force of 17 kips indicated that the moment at the interfaces was still not fully developed and slippage of the cutoff bars must have occurred.

Specimen B5

This specimen was reinforced identically to Specimen B4 with respect to the amount and arrangement of steel. Crack intiators were placed, however, at the top and bottom faces of the beam in the middle of the CIP joint.

In the first cycle, minor cracking started in the shear span and at the interfaces. During subsequent cycles cracking around the cutoff bars inside the CIP joint occurred similarly to Specimen B4. Cracking started inside the CIP joint accompanied by the widening of one of the cracks at the interfaces. As the test progressed the cracks within the CIP joint started to connect with cracks induced by the crack intiators. From Fig. 3.3(e), it is clear that considerable inelastic deformation occurred inside the CIP joint. However, failure of the specimen occurred at one of the interfaces. From the load-deflection curve, Fig. 3.2(e), the maximum shear force attained by this specimen was 16 kips, which is below that ex-

pexted if failure was to occur at the interface. It was concluded that the moment capacity at the interfaces was reduced due to the occurence of some slippage of the cutoff bars inside the CIP joint. The specimen was loaded through four cycles with maximum displacement ductility of 3. The specimen showed stable behavior through the first three cycles, after which a loss of carrying capacity was evident as accompanied by excessive pinching due to the localization of deformation at the interface.

Specimen B6

Specimen B6 was reinforced with 4#4 bars (top and bottom) in the precast concrete elements. All four bars were looped, two of them extending 4" inside the CIP joint, while the two others extended the full length of the joint, Fig. 3.1(d). Horizontal bars were placed at the corners of the loops to increase the anchorage of the bars.

At the begining of the test cracks occurred in the shear span as well as the interface locations. As the test progressed, the cracks in the shear span and at the interfaces began to widen simultaneously. Before the specimen reached yield in the second cycle, the shearing force on the beam was 22 kips, which was much higher than the anticipated force. This proved that the arrangement used in this specimen was capable of developing the full moment capacity of the interface sections and that premature failures at these locations were prevented. However, as the test went further it was clear that the primary location for inelastic activity was still at one of the interface locations. Failure occurred ultimately at one of the interface locations due to crushing of the concrete in the precast elements,

Fig. 3.3(f), and no significant deformation was visible inside the CIP joint.

From the load-deflection curve, Fig. 3.2(f), a stable behavior with no drop in the load carrying capacity was observed initially. At the conclusion of the test pinching occurred due to the localization of failure. The test specimen was loaded through three cycles with a maximum displacement ductility of 3.5.

Specimen B7

This specimen was reinforced identically to specimen B6 with respect to the amounts and arrangement of steel. However, crack intiators were placed at the top and bottom faces of the beam in the middle of the CIP joint. Because B7 was identical to B6 it was expected that the behavior would be almost the same.

In the first cycle cracks occurred in the shear span and the interface locations. As the test progressed cracks in the shear span did not increase or widen as was observed for Specimen B6. The cracks at the interfaces, however, started to pick all the deformation. Due to the existence of the crack intiator, some deformation propagated from the interface to the induced crack locations inside the CIP joint, Fig. 3.3(g). With subsequent cycles a crack at one of the interfaces began to widen and ultimate failure by crushing of the concrete in the precast elements occurred.

Specimen B7 did not reach the same shear load capacity as Specimen B6, because the deformation from the beginning of the test was concentrated at one of the interface sections. In Specimen B6 the cracks that de-

veloped in the shear span helped in distributing the deformation, thus increasing the capacity of the specimen. It can be seen from Fig. 3.2(g), that the load carrying capacity was maintained during the test. However, some pinching occurred at the end of the test due to the localization of the damage. The specimen was loaded through four cycles with a maximum ductility of 3.

Specimen B8

Specimen B8 was reinforced with 3#4 and 2#3 top and bottom bars in the precast elements. All the bars were looped together, the 3#4 bars were extended 4 in. inside the CIP joint, while the 2#3 bars were extended the full length of the CIP joint, Fig. 3.1(f). This arrangement is similar to the one used in Specimens B6 and B7. In Specimens B6 and B7 2#4 bars were extended the full length of the CIP joint, and when overlapped with the 2#4 bars from the other element, the anchorage was assumed to be sufficient to have them act as 4#4 in the middle section of the CIP joint. In Specimen B8, this effect was reduced by using 2#3 bars the full length of the CIP joint so that they would act as 4#3, which is equivalent to the design needs. Crack intiators were placed at the top and bottom faces to induce cracks inside the CIP joint. Also, the SIFCON used in this specimen was of higher strength than the ones used before.

The specimen was loaded through six cycles with a maximum displacement ductility of 6.25. As the test started, cracks occurred in the shear span and at the interfaces. As the test progressed cracks in the shear span increased in number and widened, while a crack induced by the crack intiators became visible. From the load-deflection curve, Fig. 3.2(h), it

can be seen that the behavior was excellent during the first four cycles. This was due to the well distributed crack pattern in the shear span, at the interfaces, and inside the CIP joint. However, in the last two cycles, the inelastic deformation concentrated at the crack inside the CIP joint. A significant loss in the load carrying capacity, a reduction in stiffness, and pinching occurred during the last two cycles. This was due to the localization of failure at the crack induced inside the CIP joint. Figure 3.3(h), shows the specimen at the end of the test. The specimen showed a good energy dissipation capacity and attained a higher level of ductility compared to other specimens. The shear force carried by this specimen was higher than the calculated value due to the good distribution of cracks outside the CIP joint where the load was being carried in the first two cycles before the deformation concentrated at the crack inside the CIP joint.

Specimen B9

Specimen B9 was reinforced with 4#4 top and bottom bars in the precast concrete elements. All four bars were looped, and were extended 4 in. inside the CIP joint. Closed loop 2#4 bars were put to connect the two precast elements. The details of the steel arrangements is shown in Fig. 3.1(g). This arrangement was used because of the ease and speed of construction in comparison to the previous specimens. Crack intiators were placed in the middle of the CIP joint to help induce cracking inside the joint.

Similarly to Specimen B8, this beam was loaded through six cycles with maximum displacement ductility of 6.25. During the first cycle mi-

nor cracking occurred in the shear span accompanied by cracks at the interfaces. In the second cycle a crack was visible inside the CIP joint. In subsequent cycles, all the deformation was concentrated in this crack and no more action was visible in the cracks at the interfaces, Fig 3.3(i).

From the load-deflection curve, Fig. 3.2(i), a stablity in the behavior of the specimen during the first three cycles can be observed. However, the load carrying capacity started to decrease as the test progressed. The specimen showed good energy dissipation capacity. Severe pinching and reduction in stiffness marked the general behavior of the specimen in the last four cycles due to the localization of failure at the crack induced inside the CIP joint.

Specimen B10

The reinforcement used in specimen B10 was identical to that used in Specimen B8. Crack initiators were not put in this specimen and the SIFCON used in the CIP joint was of the same strength as that used in specimens B2-B7.

Specimen B10 was loaded through four cycles and reached a maximum ductility of 3.3. In the first cycle cracks started in the shear span, the interfaces, and minor cracking was observed inside the CIP joint. In the next cycle, where the yield plateau was clearly visible, the crack at the interface was wide enough to conclude that yielding occurred there. Cracking inside the CIP joint was visible around the cutoff bars. As the test progressed, concrete at the interface started to crush while the cracks arround the cutoff bars became wider and most of the deformation was inside the CIP joint. It is worth noting that the cracks inside the CIP joint

did not start from the extreme fibers of the beam, but rather from within, Fig. 3.3(j). This indicates that the modulus of rupture of SIFCON was high enough to prevent the development of flexural cracks inside the CIP joint without the existence of crack intiators.

A significant drop in the load carrying capacity of the specimen in the last two cycles was observed in the load-deflection curve, Fig. 3.2(j). The shear force carried by the specimen indicated that the plastic hinge occurred ouside the CIP joint and steel yielded at the interface. In the last two cycles severe pinching occurred due to the localization of failure and the slip of the cutoff bars. Also, loss of stiffness occurred due to the crushing of the concrete at the interface location.

Specimen B11

Specimen B11 was reinforced with 3#4 and 2#3 top and bottom bars in the precast elements. All the bars were looped, the 3#4 bars were extended 3 in. inside the CIP joint, while the 2#3 bars were extended the full length of the CIP joint, Fig. 3.1(e). This arrangement is similar to the one used in Specimens B4 and B5. In Specimens B4 and B5, 2#4 bars were extended the full length of the CIP joint and when overlaped with the 2#4 bars from the other element, formed an anchorage strong enough to let them act as 4#4 in the middle section of the CIP joint. In specimen B11, this factor was accounted for by using 2#3 bars the full length of the CIP joint so that they would act as 4#3 bars as needed from design computations. Crack intiators were placed at the top and bottom faces in the middle of the CIP joint to help induce cracks inside the CIP joint.

At the begining of the first cycle, minor cracking in the shear span and at the interfaces occurred. As the cycle continued, cracks were induced by the crack initiators in the top and bottom faces of the beam. In the second cycle, cracks around the cutoff bars started forming and connected with the cracks formed at the top and bottom fibers inside the CIP joint. As the test progressed, an oval shape of cracks was formed, as shown in a photograph, Fig. 3.3(k), of Specimen B11 at the end of the test. With most of the deformation concentrated in this region, the test was stopped when a large drop in strength occurred.

From the load-deflection curve, Fig. 3.2(k), it is seen that there was a significant loss in the load carring capacity of the specimen, especially during the last two cycles. The specimen was loaded through four cycles, reaching a maximum displacement ductility of 4. The shear capacity was not attained because of slippage in the cutoff bars. Cracks induced by the crack initiators in the top and bottom faces of the beam were connected through cracks around the cutoff bars, rather than by a crack through the middle CIP joint, as observed in other specimens. Due to the concentration of deformation inside the CIP joint, the specimen showed better ductility. However, severe pinching and loss of stiffness marked the end of test of specimen B11.

Specimen B12

The reinforcement used in Specimen B12 was identical to that used in Specimen B8 and B10. Crack intiators were not put in this specimen and plain concrete was used in the CIP joint instead of SIFCON.

As the test began, thin cracks started in the shear span and at the interfaces. With subsequent cycles, cracks inside the CIP joint started to form. As the test progressed a crack pattern developed. Due to the nature of the steel arrangement, the plastic hinge was localized and the specimen failed by the crushing of concrete, Fig. 3.3(l). Failure came after the specimen reached its maximum load carrying capacity which indicates that there was no distribution of the load carrying mechanism, resulting in a localized failure.

From the load-deflection curve, Fig. 3.2(l), it can be observed that the specimen was loaded through three cycles, reaching a maximum displacement ductility of 2.5. After the third cycle, the strength and stiffness of the specimen decreased noticeably due to the crushing of concrete and the test was stopped.

IV EVALUATION OF TEST RESULTS

4.1 Comparison of the Theoretical and Experimental Results

In this section comparisons of the calculated and measured moments, and thus shears in each specimen are disscused. This is done to verify and illustrate the accuracy of certain analytical assumptions which had to be made to design the specimens. Two computer subroutines were developed to calculate yield and nominal moment capacities for beam sections.

In the first subroutine a linear stress distribution was used over the section when calculating the yield moment capacity. Whitney's stress block[48] was used for modeling the concrete compression block and strain hardening was ignored for the reinforcing steel (the ACI approach) when calculating the nominal moment capacity. This subroutine was used to calculate the moment capacities of sections in the precast concrete elements.

The second subroutine was based on a nonlinear analysis technique and was used to calculate the yield and the ultimate moment capacities of sections inside the CIP joint where SIFCON was utilized. This subroutine used three different stress-strain models. First, a model for the stress-strain relationship of SIFCON in compression. Second, a model for the

stress-strain relationship for the reinforcing steel based on Sargin's approach[39]. Third, a model to charactarize the stress strain relationship of SIFCON in tension.

Table 4.1, gives the computed and measured moments for the beam sections at the interfaces. Columns two and four give the moments computed using the first subroutine. Columns three and five give the actual measured moments during testing. From columns six and seven, which compare calculated and measured moments, it can be seen that for Specimens B1 through B5, although failure occurred at the interfaces, the measured moments did not reach the calculated capacities. It is therefore assumed that slippage of reinforcement occurred. For Specimens B6 and B7, where failure also occurred at the interfaces, the actual and computed results reasonably agreed. This indicated that the reinforcement inside the CIP joint was well developed to exhibit the full moment capacities at the interfaces. It is seen also that for Specimens B8 through B12 the steel did not yield at the interface locations which means that yielding occurred inside the CIP joint. Specimen B8 reached its ultimate capacity at the interface location, although failure occurred inside the CIP joint. This explains the good behavior of this specimen which was attributed to the good distribution of inelastic deformation.

Similarly Table 4.2 gives the computed and the measured moments of beam sections inside the CIP joint. In specimens where failure occurred inside the CIP joint, noticeable discrepancy between the calculated and the measured values occurred. In Specimen B8 this can be explained as a result of the distribution of cracking in the beam. However, in Specimen B9 this indicates that the assumptions made when calculating the

moment capacities of the CIP joint, especially the yield moment, need to be revised.

Due to the size of the specimens, and accordingly the size of the CIP joint, it is believed that without crack initiators the rupture capacity of SIFCON sections was not attained, producing failure at the interfaces. This can be seen if we compare Specimens B8 (Fig. 3.3(h)) and B10 (Fig. 3.3(j). Both specimens were identicallty reinforced, however, crack initiators in the CIP joint were put in Specimen B8. Even though Specimen B8 had a higher strength SIFCON matrix, failure occurred inside the CIP joint. For Specimen B10 failure occurred at the interface after cracking inside the CIP joint resulting from slippage of cutoff bar.

4.2 Evaluation of Test Results

To better understand the performance of each specimen and to assess the overall results of the experimental program, a general comparison should be made among all the specimens.

The basic objective of this investigation was to arrive at an acceptable cast-in-place connection between two precast elements, which will be designed to accomodate a plastic hinge within its premises and which exhibits high energy dissipation capacity and large ductility. In this study the variables were the steel arrangements inside the CIP joint, and the existence of crack intiators in the top and the bottom fibers inside the CIP joint to help induce cracks inside the connector element. The SIFCON matrix was expected to provide sufficient strength and ductility as needed.

The specimens in this study showed different failure locations depending on the steel arrangement used. The effect of the failure location on the behavior of a particular specimen can be judged by comparing the energy dissipation for equivalent ductilities. Normalized energy dissipation for all specimens is given in Table 4.3. It can be seen that the energy dissipated by specimens where failure occurred inside the CIP joint was higher than the energy dissipated by specimens where failure occurred at the interfaces. This can also be attributed to the fact that specimens where plastic hinges occurred inside the CIP joint were more ductile and sustained more cycles than those where failure occurred outside the CIP joint.

The maximum applied load to the specimen at each cycle was compared to the maximum applied shear computed from the first yield cycle, and their ratio was used to compare the deterioration of the load carrying capacity for different specimens. The values of this ratio at different yield cycles are given in Table 4.4. It is observed that a loss in the load carrying capacity of all specimens occurs towards the end of the test. Specimens B8 and B9, which successfully survived the sixth cycle, eventually suffered a loss in the load carrying capacity when inelastic deformations were concentrated in one crack inside the CIP joint.

A comparison of the hysteresis loops, Figs 3.2 and the shear forces attained by each specimen (given in Table 4.5) provided an additional insight into the behavior of all specimens. It was apparent for Specimen B1 that the shear capacity was lower than anticipated, indicating a slippage of the cutoff bars. As a result, failure occurred at the interfaces. Therefore Specimens B2 through B7 were poured and tested with different steel configurations to assess the development of the cutoff bars, and to reach a

satisfactory arrangement that will ensure a plastic hinge inside the CIP joint.

From the results of Specimens B2 through B7 it was clear that the steel arrangement for Specimens B6 and B7 was the best for developing the full moment capacity of the sections at the interface locations. The test results of B2 and B3 indicated that the development length of the straight cutoff bars was insufficient to ensure the full expected moment capacity at the interface locations. This conclusion was drawn because the measured shear forces was lower than expected. Specimens B4 and B5 indicated that looping cuttoff bars increased their anchorage. However, their extension inside the CIP joint were not sufficient enough to prevent slippage from occurring.

It can also be observed from the test results of B6 and B7 that, although the moment capacity was developed at the interface sections, failure still occurred at these sections rather than inside the CIP joint. This is believed to be due to the overlapping of the reinforcement which was fully extended inside the CIP joint. Thus, the anchorage of the steel bars was increased significantly so that they acted as 4#4 bars rather than 2#4 as expected. Given this behavior and given the existence of a natural weak points (the interfaces) in the beams, the failure occurred at the interface sections.

To eliminate the above discribed effects, Specimens B8, B10, B11, and B12 were reinforced with 3#4 and 2#3 top and bottom bars in the precast elements, with the 2#3 looped bars extended the full length of the

joint. This provided a section at the middle of the CIP joint with 4#3 bars which is equivalent to 2#4 as initially designed.

To be able to rank all the specimen, four criteria were used to classify the performance of each specimen. Table 4.6 gives the performance of each specimen in terms of the CIP joint condition, the location of failure, the normalized energy dissipation capability, whether steel yielding occurred at the interfaces, and the occurrence or non-occurrence of slippage in the longitudinal reinforcement at the interface sections.

V SUMMARY AND CONCLUSION

4.1 Summary of the Test Results

The use of precast concrete in areas of high seismicity depends primarily on the development of a strong, ductile, and a good energy dissipating connector between precast elements. The objective of this ongoing research is to develop such a connector for precast or precast prestressed concrete beam-column subassemblages. Moreover, such a connector, which will be placed away from the column face, will be designed so that a plastic hinge occurs at the connector location during load reversals. The main objective of the reported investigation, however, is to find an acceptable steel configuration inside the connector to achieve a plastic hinge there. The matrix used in this connector is SIFCON, a material which possess high ductility and good energy dissipation.

To acomplish this objective, twelve beam assemblages were constructed. The assemblages consisted of two precast concrete elements connected together to form a beam with a cast-in-place (CIP) joint using SIFCON as the matrix in the joint. Different steel arrangements were tried aiming at developing a hinging zone inside the CIP joint. The primary variables which studied were the steel arrangements inside the CIP joint

and the presence or absence of crack intiators at the top and bottom faces of the specimens.

During testing the specimen were simply supported in the upward as well as the downward directions and were subjected to reversed loading. The points of load applications were located in the middle third of the beams. The specimens were displaced through a predifined loading history. The first loading cycle for most of the specimens was applied to determine the displacement at which yielding occurred. This was followed by load cycles at larger displacements until failure. A continuous plot of the load vs. the load point deflection was recorded during the test.

Basically there were four flexural failure locations: 1) outside the CIP joint, 2) the interface between the CIP joint and the precast segments, 3) inside the CIP joint with the steel yielding at the interface, and 4) inside the CIP joint with no steel yielding at the interfaces.

The ultimate objective of this study was reached, for two of the combinations of variables, when the plastic hinge formed inside the CIP joint while the moment capacity at the interface was maintained at a desirable level.

4.2 Conclusion

Based on the results of the tweleve specimens tested in this investigation the following conclusions can be drawn.

1. The existence of a crack intiator was important to induce cracks inside the CIP joint. This conclusion, however, is dependent on the size of the specimens and the CIP joints and is

only applicable to the size investigated in this study. Further investigations are needed to determine the generality of this conclusion.

2. The looping of the steel vertically inside the CIP joint increased the anchorage of the bars in SIFCON. For the successful arrangements (arrangements D' & E'), the looping of the steel helped in developing the full moment capacities at the interfaces and prevented any slippage of the cutoff bars when sufficiently extended inside the CIP joint.

3. Athough the two most successful specimens (B8,B9) had localized failure, SIFCON showed good ductility and energy dissipation capabilities. The localized failure, however, was responsible for stiffness degradation and pinching. The manipulation of the ratio of the moment capacities btween sections inside and outside the CIP joint could produce a better deformation distribution and thus, a better behavior.

4.3 Needed research

Although this study proved that providing a strong and ductile connector and also creating a plastic hinge inside this connector is achievable, several research topics need to be further investigated.

1. There is need to study full size beams and determine the effect of size on the behavior in general.

2. There is need to determine whether crack intiators are needed or not in full scale structures.

3. There is need to further investigate the use of different steel configurations to try to distribute the deformation inside the CIP joint.

4. Further investigation is needed to determine the effect of the ratio of moment capacities between sections inside the CIP joint and the interfaces, and whether yielding at the interfaces should be permited in order to distribute deformations.

5. There is need to extend the range of FRC composite materials for the matrix of the CIP joint matrix to see if a reliable, strong, and ductile connector can be further developed.

REFERENCES

1. Abdel-Fattah, B.A., and Wight, J.K., "Experimental Study of Moving Plastic Hinging Zones for Earthquake Resistant Design of Reinforced Concrete Buildings", Report No. UMCE 85-11, Department of Civil Engineering, The University of Michigan-Ann Arbor, December 1985.

2. ACI Committee 544, "State-of-the-Art Report on Fiber Reinforced Concrete", American Concrete Institute, Detroit, 1984.

3. ATC-8 Seminar, "Design of Prefabricated Concrete Buildings For Earthquake Loads", Proceedings, ATC, Berkeley, California, January 1982.

4. Batson, G., Jenkins, E., and Spatney, R., "Steel Fibers as Shear Reinforcement in Beams", ACI Journal, Vol. 69, October 1972.

5. Balaguru, p., and Ezeldin, A., " Behavior of Partially Prestressed Beams made with High Strength Fiber Concrete", Fiber Reinforced Concrete-Properties and Applications, SP-105, ACI, Detroit, 1987.

6. Bertero, V.V., and Popov, E .P., "Seismic Behavior of Ductile Moment Resisting Reinforced Concrete Frames", Reinforced Concrete Structures in Seismic Zones, ACI Publication SP-53, ACI, Detroit, MI, 1977.

7. Bishara, A. G., and Brar, G. S., "Rotational Capacity of Prestressed Concrete Beams", Journal of the Structural Division, ST 9, September 1974.

8. Blakeley, R.W., and Park, R., "Prestressed Concrete Sections With Cyclic Flexure", Journal of the Structural Division, ASCE, V. 99, August 1973.

9. Blakeley, R.W., and Park, R., "Seismic resistance of Prestressed Concrete Beam-Column Assemblies", ACI Journal, V. 68, September 1971.

10. "Building Code Requirements for Reinforced Concrete", (ACI 318-83), Committee 318, American Concrete Institute, Detroit, Michigan, 1983.

11. Clough, D. P., "Design of Connectors For Precast Prestressed Concrete Buildings for the Effects of Earthquakes", Technical Report No. 5, PCI, March 1985.

12. "Code of Practice for the Design of Concrete Structures", NZS 3101:1982, Standard Association of New Zealand, Wellington, New Zealand.

13. Craig, R. J., McConnell, J., Germann, H., Dib, N., and Kashani, F., "Behavior of Reinforced Fibrous Concrete Columns", Symposium on Fiber Reinforced Concrete, ACI Special Publication, SP-81, ACI, Detroit, 1984.

14. Craig, R. J., Mahadev,S., Patel, C.C., Viteri, M., and Kertesz, C., "Behavior of Joints Using Reinforced Fibrous Concrete", Symposium on Fiber Reinforced Concrete, ACI Special Publication, SP-81, ACI, Detroit, 1984.

15. Craig, R. J., "Structural Applications of Reinforced Fibrous Concrete", Concrete International Journal, Vol. 6, No. 12, ACI, December 1984.

16. Dolan, C., Stanton, J., and Anderson, R., "Moment Resistant Connections and Simple Connections", PCI Journal, Vol. 32, Mar.-Apr. 1987.

17. Durani, A.J., and Wight, J.K., "Experimental and Analytical Studies of Interior Reinforced Concrete Beam-to-Column Connections", Report No. UMEE 82R3, Department of Civil Engineering, The University of Michigan, Ann Arbor, Michigan, July 1982.

18. Englekirk, R., "Concepts for the Development of Earthquake Resistant Ductile Frames of Precast Concrete", PCI Journal, Vol. 32, Jan.-Feb. 1987.

19. Englekirk, R., "Overview of ATC Seminar on Design of Prefabricated Concrete Buildings For Earthquake Loads", PCI Journal, Vol. 27, Jan.-Feb. 1982.

20. Hamahara, M., Suetsugu, H., and Motooka, J., "Effect of Average Prestress in Concrete on Ductilities of Prestressed Concrete Flexural Members", Proceedings, The 10th International Congress of the FIP, New Delhi, FEB. 1986.

21. Hawkins, N., and Englekirk, R., "US-Japan Seminar on Precast Concrete Construction in Seismic Zones", PCI Journal, Vol. 32, Mar.-Apr. 1987.

22. Henager, C. H., "Steel Fibrous, Ductile Concrete Joint For Seismic-Resistant Structures", Symposium on RC Structures in

Seismic Zones, ACI Special Publication, SP-53, ACI, Detroit, 1974.

23. Homrich, J., and Naaman, A.E., " Stress-Strain Properties of SIFCON in Compression", Fiber Reinforced Concrete-Properties and Applications, SP-105, ACI, Detroit, 1987.

24. Jindal, R., and Sharma, V., " Behavior of Steel FIber Reinforced Concrete Knee-Type Beam-Column Connections", Fiber Reinforced Concrete-Properties and Applications, SP-105, ACI, Detroit, 1987.

25. Jindal, R., Hassan, K., "Behavior of Joints Using Reinforced Fibrous Concrete", Symposium on Fiber Reinforced Concrete, ACI Special Publication, SP-81, ACI, Detroit, 1984.

26. Jindal, R. L., "Shear and Moment Capacities of Steel Fiber Reinforced Concrete Beams", Symposium on Fiber Reinforced Concrete, ACI Special Publication, SP-81, ACI, Detroit, 1984.

27. Lankard, D. R., "Properties, Applications: Slurry Infiltrated Fiber Concrete (SIFCON)", Concrete International Journal, Vol. 6, No. 12, ACI, December 1984.

28. Lee, D.L., Wight, J.K., and Hanson, R.D., "Reinforced Concrete Beam-Column Joints Under Large Load Reversals", Report No. UMEE 76S4, Department of Civil Engineering, The University of Michigan, Ann Arbor, Michigan, May 1976.

29. Meinheit, D.F., and Jirsa, J.O., "The Shear Strength of Reinforced Concrete Beam-Column Joints", Report No. 77/1, Department of Civil Engineering, Structures Res. Lab., University of Texas at Austin, January 1977.

30. Milburn, J.R., and Park, R., "Behavior of Reinforced Concrete Beam-Column Joints Designed to NZS 3101", Report No. 82-7, Department of Civil Engineering, University of Canterbury, Cristchurch, New Zealand, Febuary 1982.

31. Nishioka, K., Kakimi, N., Yamakawa, S., Shirakawa, K., "Effective Applications of Steel Fiber Reinforced Concrete", RILEM Symposium 1975, Fiber Reinforced Cement Concrete, Vol. 1, The Construction Press Ltd. 1975.

32. Park, R., and Bull, D., "Seismic Resistance of Frames Incorporating Precast Prestressed Concrete Beam Shells", PCI Journal, Vol. 31, Jul.-Aug. 1986.

33. Paulay, T., and Park, R., "Joints in Reinforced Concrete Frames Designed for Earthquake Resistance", Report No.84-9, Department of Civil Engineering, Univesity of Canterbury, Cristchurch, New Zealand, June 1984.

34. Penzien, J., "Damping Charactaristics of Prestressed Concrete", ACI Journal, September 1964.

35. Popov, E.P., "Seismic Behavior of Structural Subassemblages", Journal of the Structural Division, ASCE Proceedings, Vol. 106, No. ST7, July, 1980.

36. Popov, E .P., and Bertero, V.V., and Galunic, B., "An Approach for Improving seismic Behavior of Reinforced Interior Joints", Report No. EERC-77/30, The University of California-Berkeley, December 1977.

37. Popov, E .P., and Bertero, V.V., "Hysteretic Behavior of Ductile Moment Resisting Reinforced Concrete Frame

Components", Report No. EERC-75/16, The University of California-Berkeley, April 1975.

38. "Recommendations for the Design of Beam-Column Joints in Monolitic reinforced Concrete Structures", ACI-ASCE Joint Committee 352, Journal of the ACI, Proceedings, V.82, No. 3, May-June 1985.

39. Sargin, M., " Stress-Strain Relationship for Concrete and the Analysis of Structural Concrete Sections", Study No. 4, Solid Mechanics Division, University of Waterloo, Ontario, Canada, 1971.

40. Scribner, C.F., and Wight, J.K., "Delaying Shear Strength Decay in Reinforced Concrete Flexural Members Under Large Load Revrsals", Report No. UMEE 78R2, Department of Civil Engineering, The University of Michigan, Ann Arbor, Michigan, May 1978.

41. Sood, V., and Gupta, S., " Behavior of Steel Fibrous Concrete Beam-Column Connections", Fiber Reinforced Concrete-Properties and Applications, SP-105, ACI, Detroit, 1987.

42. Susuki, K., and Nakatsuka, T., "Ductile Behavior of Partially Prestressed Concrete Beams with Confined Concrete Under Scores of High Intensity Cyclic Loading", Proceedings, The 10th International Congress of the FIP, New Delhi, FEB. 1986.

43. Susuki, K., Nakatsuka, T., and Cai, J., "Behavior and Hysteresis Charactaristics of Partially Prestressed Concrete Columns with Circular Spiral Reinforcement", The 10th International Congress of the FIP, New Delhi, FEB. 1986

44. Thompson, K.J., and Park, R., "Ductility of Prestressed and Partially Prestressed Concrete Beam Sections", PCI Journal, V. 25, Mar.-Apr. 1980.

45. Thompson, K.J., and Park, R., "Seismic Response of Partially Prestressed Concrete", Proceedings, ASCE, V. 106, ST8, Aug. 1980.

46. Uniform Building Code, 1982 Edition, International Confference of Building Code Officials, Wittier, California, 1982.

47. US-Japan Seminar, "Precast Concrete Construction in Seismic Zones", Proceedings, Vol. 1 & 2, Tokyo, Japan, October 1986.

48. Whiteny, C.S., "Plastic Theory of Reinforced Concrete Design", Trans. ASCE, vol. 107, 1942.

Table 2.1 PARAMETRIC DETAILS

Specimen Number	Design ratio of the moment outside the CIP joint to be used inside the CIP	Criterion ouside the CIP Joint	Crack Intiator	Steel Arrangement
B1	0.63	Ma < My	With	A
B2	0.63	Ma < My	Without	B
B3	0.63	Ma < My	With	B
B4	0.63	Ma < My	Without	C
B5	0.63	Ma < My	With	C
B6	0.63	Ma < My	Without	D
B7	0.63	Ma < My	With	D
B8	0.73	Ma < My	With	D
B9	0.63	Ma < My	With	E
B10	0.63	Ma < My	Without	D
B11	0.63	Ma < My	With	C
B12*	0.63	Ma < My	Without	D'

* In this Specimen concrete was used as the matrix for the CIP joint.

TABLE 2.2 REINFORCEMENT DETAILS

Specimen Number	Reinforcement Provided		Steel Arrangements
	Outside CIP Joint	Inside CIP Joint	
B1	4 #4	2 #4	A
B2	4 #4	2 #4	B
B3	4 #4	2 #4	B
B4	4 #4	2 #4	C
B5	4 #4	2 #4	C
B6	4 #4	2 #4	D
B7	4 #4	2 #4	D
B8	3 #4 + 2 #3	4 #3	D'
B9	4 #4	2 #4	E
B10	3 #4 + 2 #3	4 #3	D'
B11	3 #4 + 2 #3	4 #3	C'
B12	3 #4 + 2 #3	4 #3	D'

Table 2.3 SIFCON TRIAL MIXES

Mix #	Cement	Sand*	Water	Fly Ash	Additives
1	1	-	1	1	Melement (liquifier) if needed (max 2% by wt. of cement)
2	1	1.5	0.8	-	
3	1	2	.6	-	
4	1	2	.5	-	
5	1	3	.9	-	

* Ottawa Sand type C-109

Table 2.4 MATERIAL PROPERTIES

Specimen Number	Matrix Compressive Strength	
	Outside CIP Joint (Concrete)	Inside CIP Joint (SIFCON)
B1	5800	4400
B2	6200	4200
B3	6200	4200
B4	6200	4350
B5	6200	4350
B6	6200	4400
B7	6200	4400
B8	6300	5200
B9	6300	4550
B10	6300	4550
B11	6300	4550
B12	5800	5100

Bar size	Grade	Yield
# 3/16		79
# 3	60	73.5
# 4	60	76

TABLE 3.1 DISPLACEMENT DUCTILITIES

Specimen Number	Displacement of each Cycle Relative to the Yield Cycle					
	Cycle Numbers*					
	1	2	3	4	5	6
B1	0.5	1	2	3	4	-
B2	0.5	1	2	3	3.5	-
B3	0.5	1	2	3	3.7	-
B4	1	1.75	2.5	3.5	-	-
B5	0.5	1	2	3	-	-
B6	0.5	1	2	3	-	-
B7	0.5	0.75	2	3	-	-
B8	0.5	1	2.5	3.75	5	6.25
B9	1	1.5	2.8	4	5.3	6.25
B10	1	2	2.8	3.3	-	-
B11	1	12	3	4	-	-
B12	0.5	1	2	2.5	-	-

* See Fig. 3.2 for Cycle Sequence

TABLE 4.1 CALCULATED AND ACTUAL YIELD AND MAXIMUM MOMENTS OUTSIDE THE CIP JOINT *

Specimen Number	Yield Moment k-in		Maximum Moment k-in		Mya / Myn	Ma / Mm
	Calculated Myn	Actual Mya	Calculated Mm	Actual Ma		
B1	460	250	470	260	0.54	0.58
B2	460	350	470	375	0.76	0.8
B3	460	440	470	440	0.95	0.93
B4	460	360	470	425	0.78	0.9
B5	460	375	470	400	0.82	0.85
B6	460	500	470	550	1.08	1.17
B7	460	440	470	490	0.95	1.03
B8	465	415	475	475	0.89	1
B9	460	340	470	350	0.73	0.64
B10	465	460	475	460	0.99	0.97
B11	465	260	475	275	0.56	0.57
B12	465	290	475	325	0.62	0.68

* Using the ACI approach

TABLE 4.2 CALCULATED AND ACTUAL YIELD AND MAXIMUM MOMENTS INSIDE THE CIP JOINT *

Specimen Number	Yield Moment k-in		Maximum Moment k-in		Mya / Myn	Ma / Mm
	Calculated Myn	Actual Mya	Calculated Mm	Actual Ma		
B1	245	250	300	260	1.02	0.875
B2	245	350	300	375	1.43	1.25
B3	245	435	300	435	1.78	1.46
B4	245	360	300	425	1.48	1.42
B5	245	375	300	400	1.53	1.33
B6	245	500	300	550	2.04	1.83
B7	245	440	300	485	1.79	1.63
B8	280	415	350	475	1.48	1.36
B9	245	340	300	350	1.38	1.16
B10	245	460	300	460	1.88	1.54
B11	245	260	300	275	1.07	0.92
B12	230	290	275	325	1.25	1.19

* Using the ACI approach

TABLE 4.3 ENERGY DISSIPATION OF THE SPECIMENS

Specimen Number	Ratio of the Energy Dissipation of each Cycle to that of the First Yield Cycle					
	Load Cycle Numbers					
	1	2	3	4	5	6
B1	0.22	1	2.33	2.29	2.33	-
B2	0.31	1	3.94	5.8	3.12	-
B3	0.24	1	4.75	6.29	5.24	-
B4	1	2.32	3.27	4.36	-	-
B5	0.28	1	3.41	4.83	-	-
B6	0.28	1	3.77	5.65	-	-
B7	0.2	0.33	2.3	4.22	-	-
B8	0.31	1	4.87	7.87	10	4.82
B9	1	1.25	3.6	5.18	6.2	7.8
B10	1	2.45	2.52	2.51	-	-
B11	1	2	2.23	2.61	-	-
B12	0.2	1	2.04	0.72	-	-

TABLE 4.4 CYCLIC LOAD CARRYING CAPACITY OF THE SPECIMENS

Specimen Number	Ratio of the Maximum Load at each Cycle to that of the First Yield Cycle					
	Load Cycle Numbers					
	1	2	3	4	5	6
B1	0.86	1	0.85	0.7	0.67	-
B2	0.73	1	0.97	0.83	0.77	-
B3	0.6	1	0.97	0.77	0.71	-
B4	1	1.17	1.14	1	-	-
B5	0.73	1	1.07	0.9	-	-
B6	0.58	1	1.19	1.22	-	-
B7	0.61	0.87	1.19	1.16	-	-
B8	0.69	1	1.15	1.15	0.97	0.64
B9	1	1.12	1.17	1.04	1	0.92
B10	1	0.97	0.73	0.57	-	-
B11	1	0.96	0.74	0.65	-	-
B12	0.77	1	1.04	0.73	-	-

TABLE 4.5 SHEAR FORCES

Specimen Number	Calculated Shear Forces in kips if Flexural Failure is to Occur		Max. Measured Shear Forces in kips
	Outside CIP Joint	Inside CIP Joint	
B1	18.5	12	10.5
B2	18.5	12	15
B3	18.5	12	17.5
B4	18.5	12	17
B5	18.5	12	16
B6	18.5	12	22
B7	18.5	12	19.5
B8	19	14	19
B9	18.5	12	14
B10	19	12	18.5
B11	19	12	12
B12	19	12	13

TABLE 4.6 OVERALL PERFORMANCE

Specimen Number	CIP joint Condition at the end of Test	Location of the Plastic Hinge	Normalized Total Energy Dissipated *	Yielding Outside the CIP joint	Slip of cutoff bars inside the CIP joint	Rank
B1	Damaged	Interface	8.2	Yes	Yes	12
B2	Intact	Interface	14.2	Yes	Yes	11
B3	Intact	Interface	17.5	Yes	Yes	10
B4	Damaged	Interface	10.9	Yes	Yes	8
B5	Damaged	Interface	9.5	Yes	Yes	9
B6	Intact	Interface	10.6	Yes	Yes	6
B7	Damaged	Interface	7.6	Yes	Yes	7
B8	Damaged	CIP	28.3	Yes	Yes	1
B9	Damaged	CIP	25	No	Yes	2
B10	Damaged	Interface	8.5	Yes	Yes	3
B11	Damaged	CIP	7.9	No	Yes	4
B12	Damaged	CIP	3.95	No	Yes	5

* Normalized to the energy dissipated in the first yield cycle

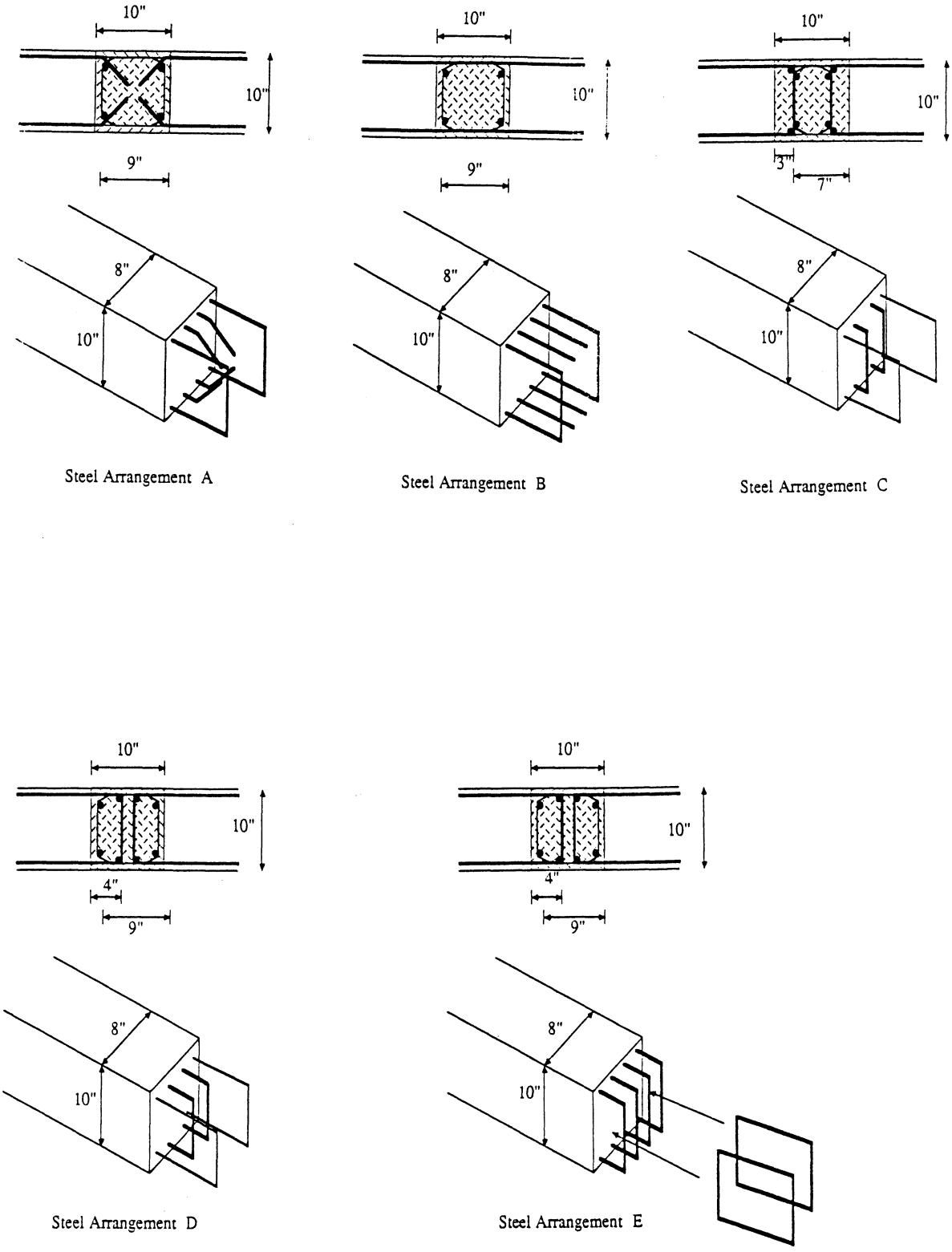

Fig. 2.1- Reinforcement configuration in CIP connections tested with beam type specimens

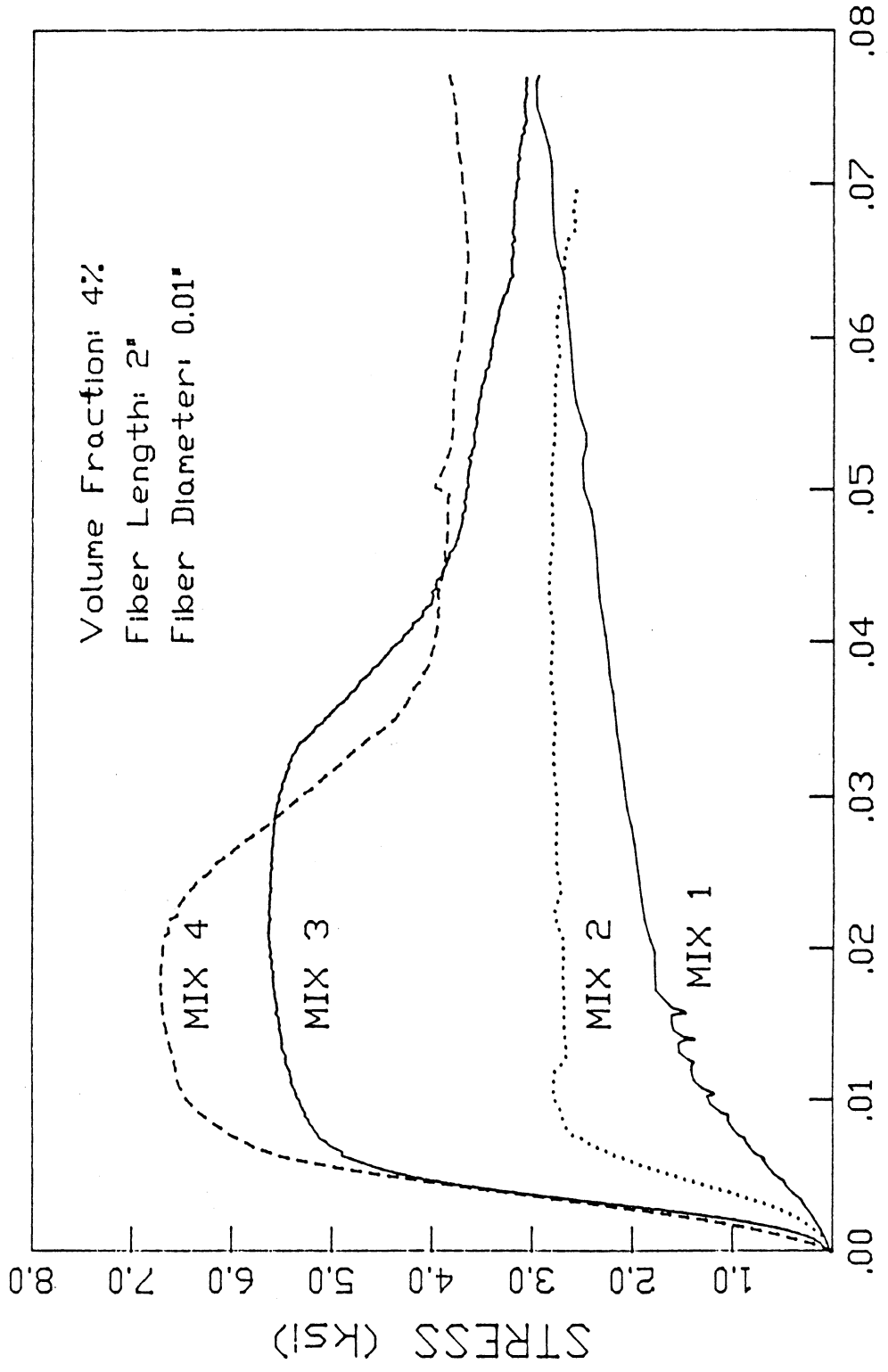

Fig. 2.2- Stress-Strain curves for SIFCON trial mixes under compression loading

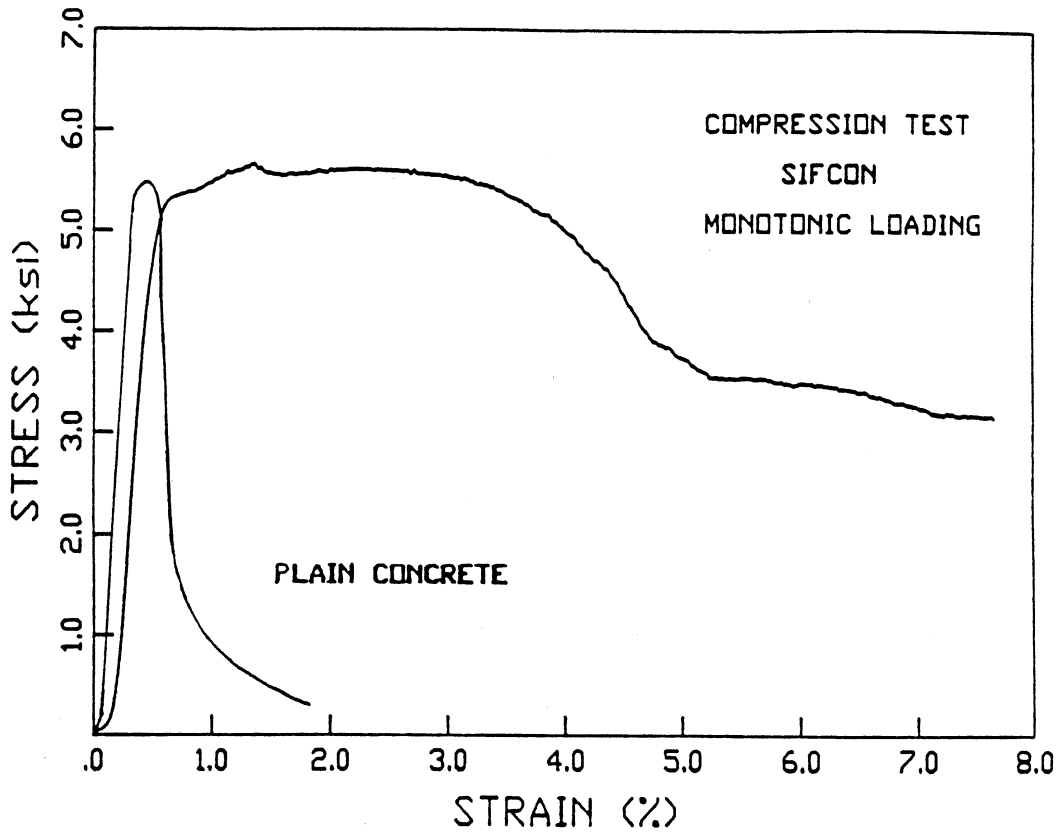

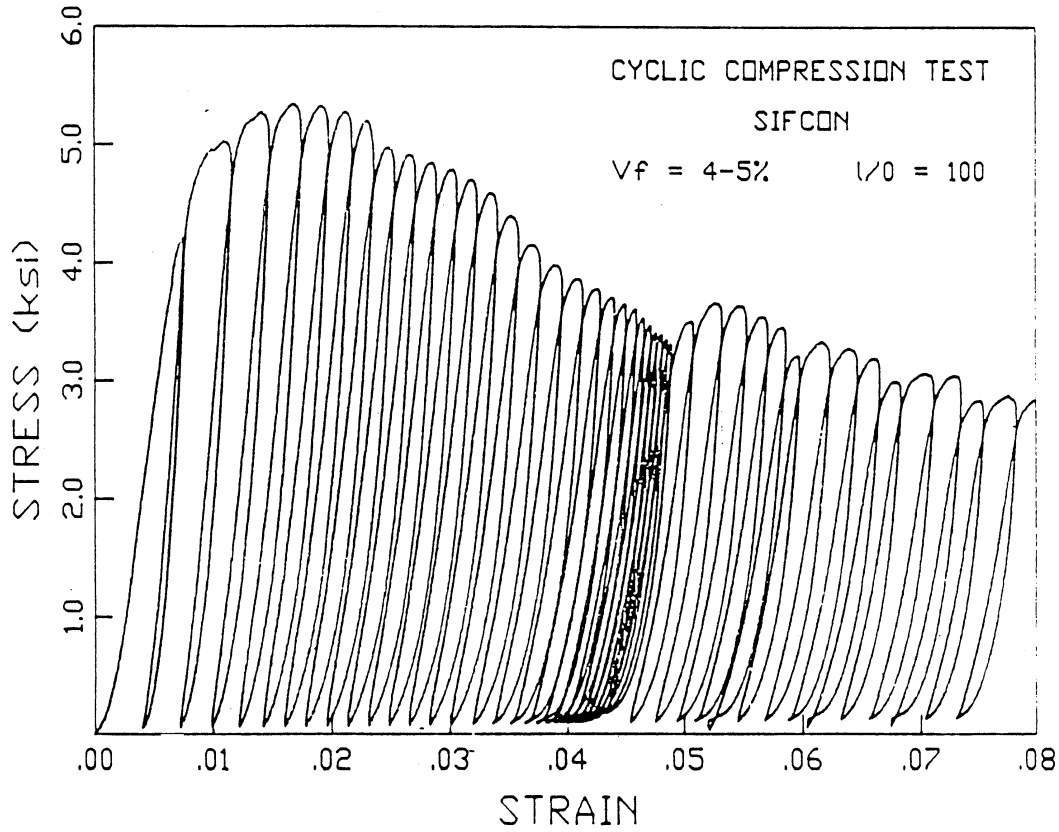

Fig. 2.3- (a) Typical stress-strain response to monotonic loading for the SIFCON mix.
(b) Typical stress-strain response to cyclic loading for the mix.

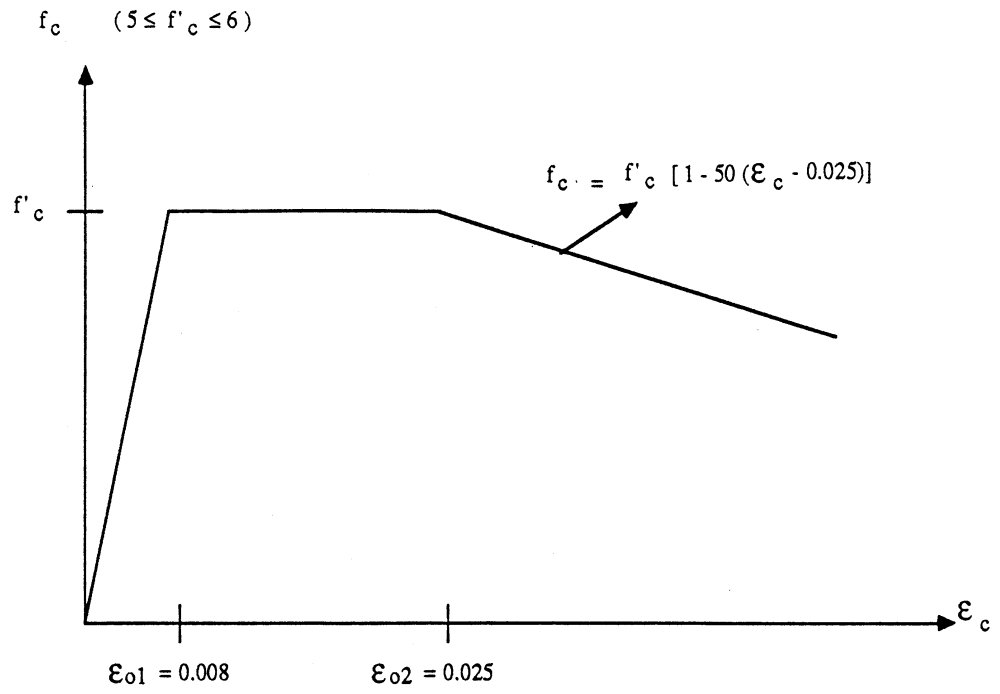

Fig. 2.4- Stress-Strain model of the SIFCON material under compression.

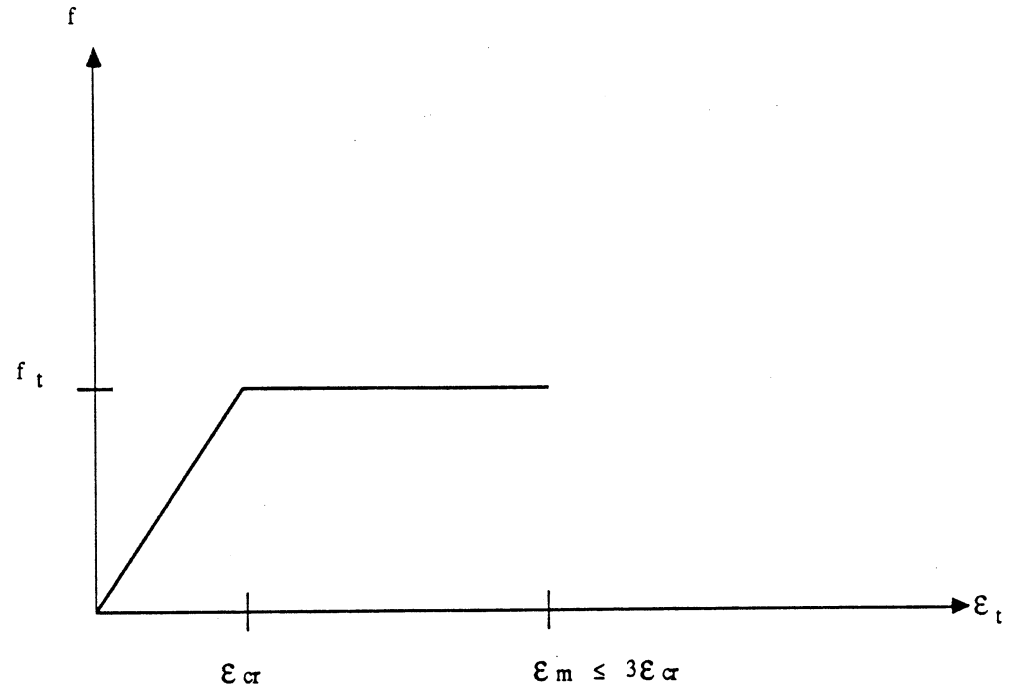

Fig. 2.5- Stress-Strain model of the SIFCON material under tension.

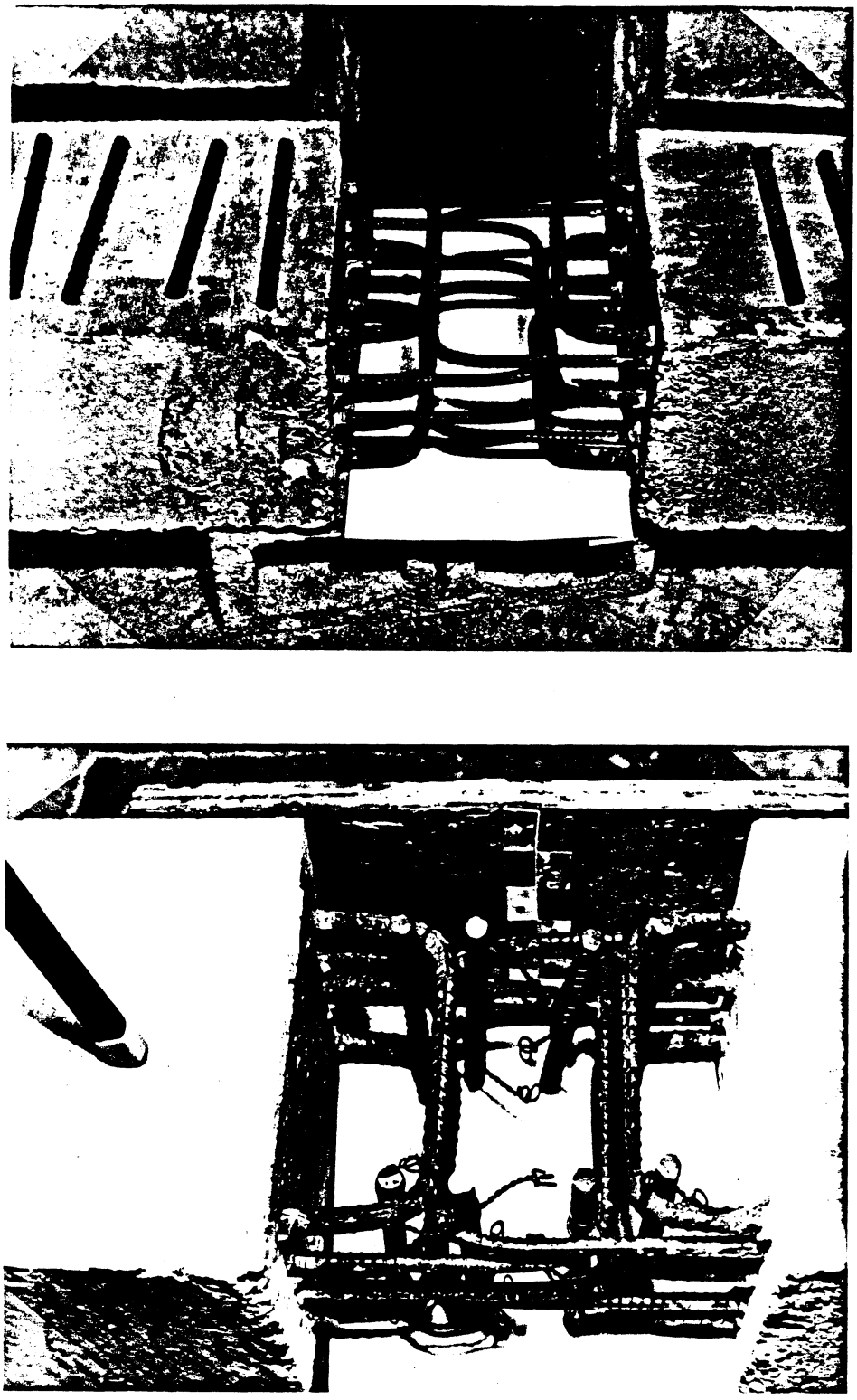

Fig. 2.6- (a) The assembly of the precast elements.

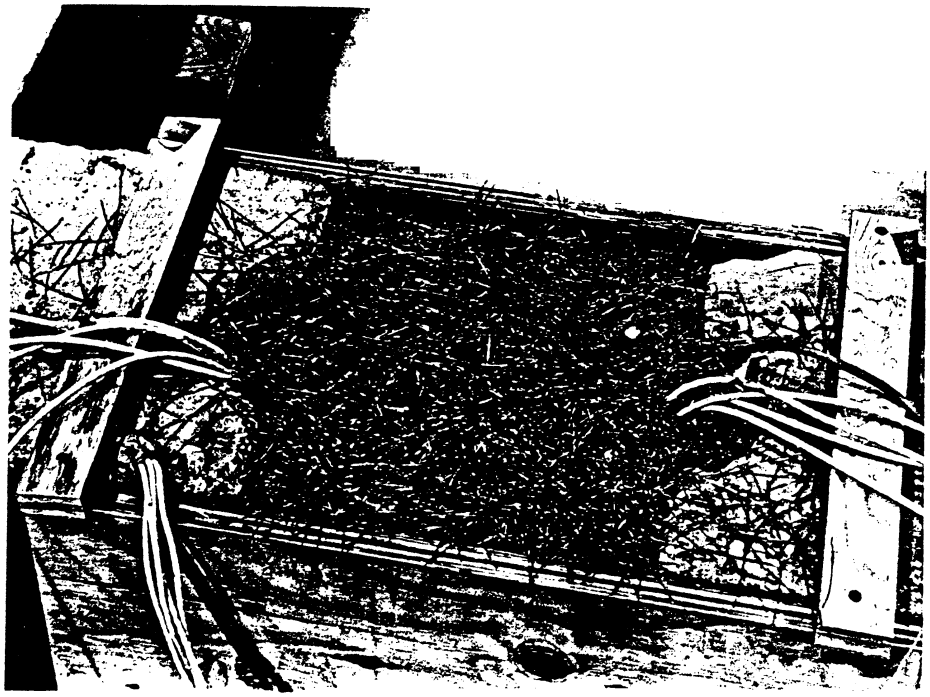

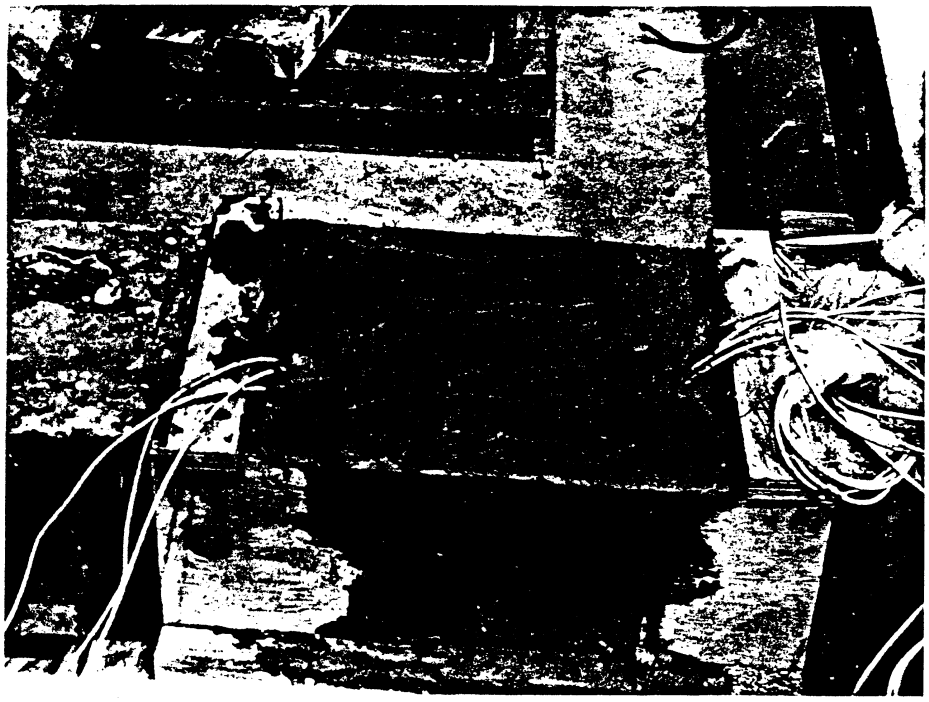

Fig. 2.6- (b) The placing of fibers and the SIFCON joint after pouring the slurry.

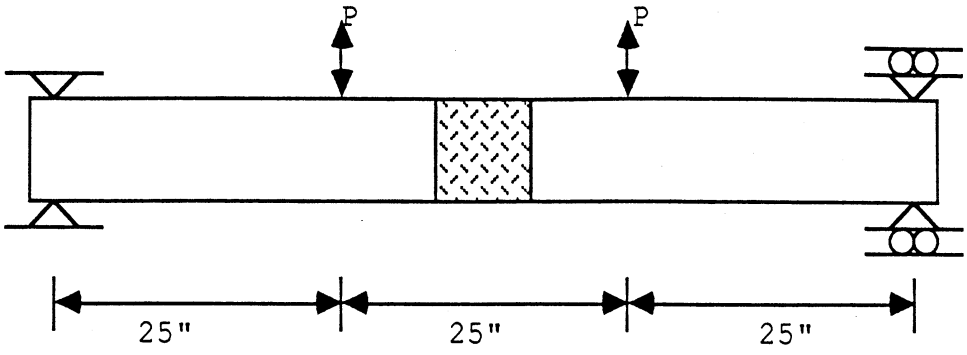

Fig. 2.7- Beam type configuration and testing set-up.

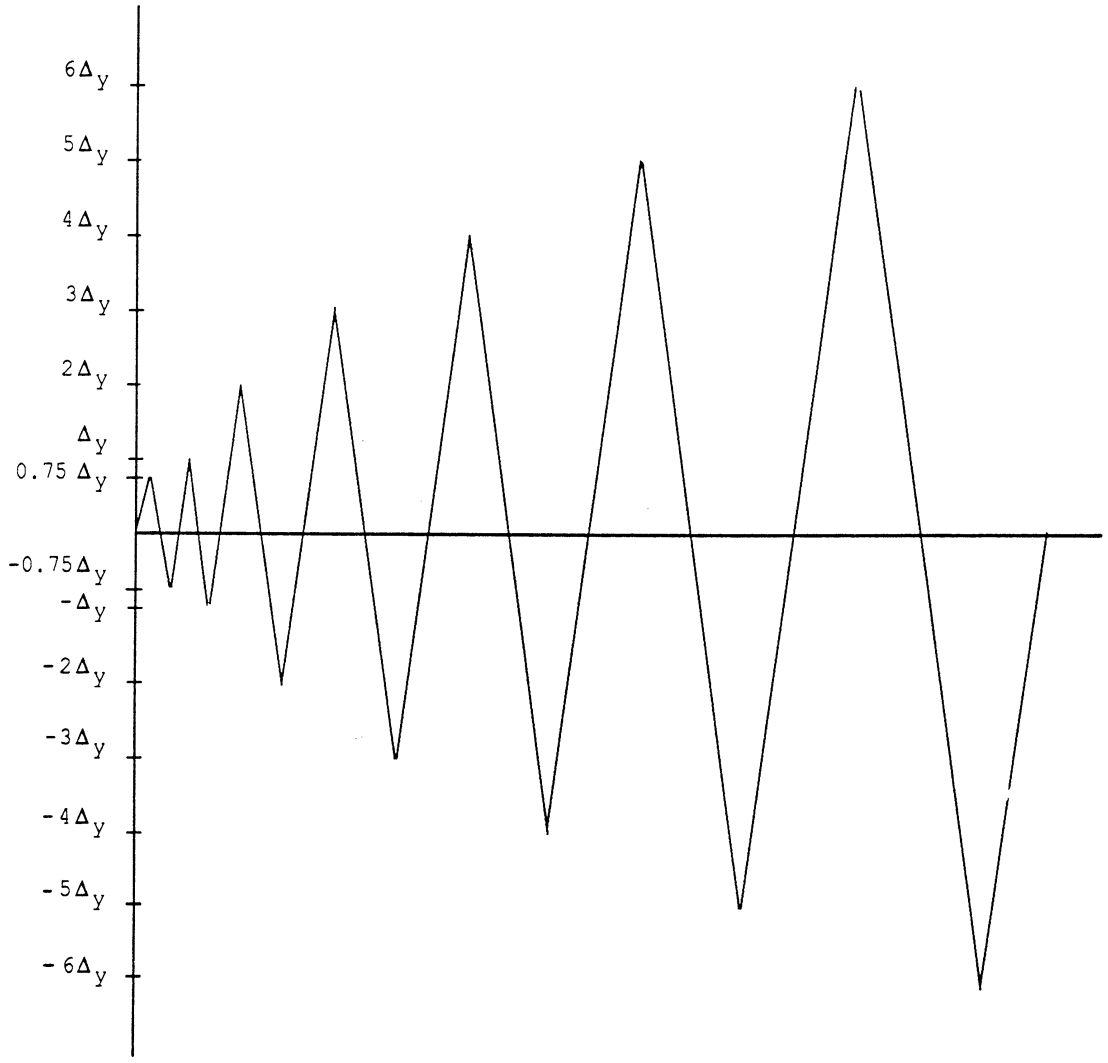

Fig. 2.8- Displacement control loading sequence.

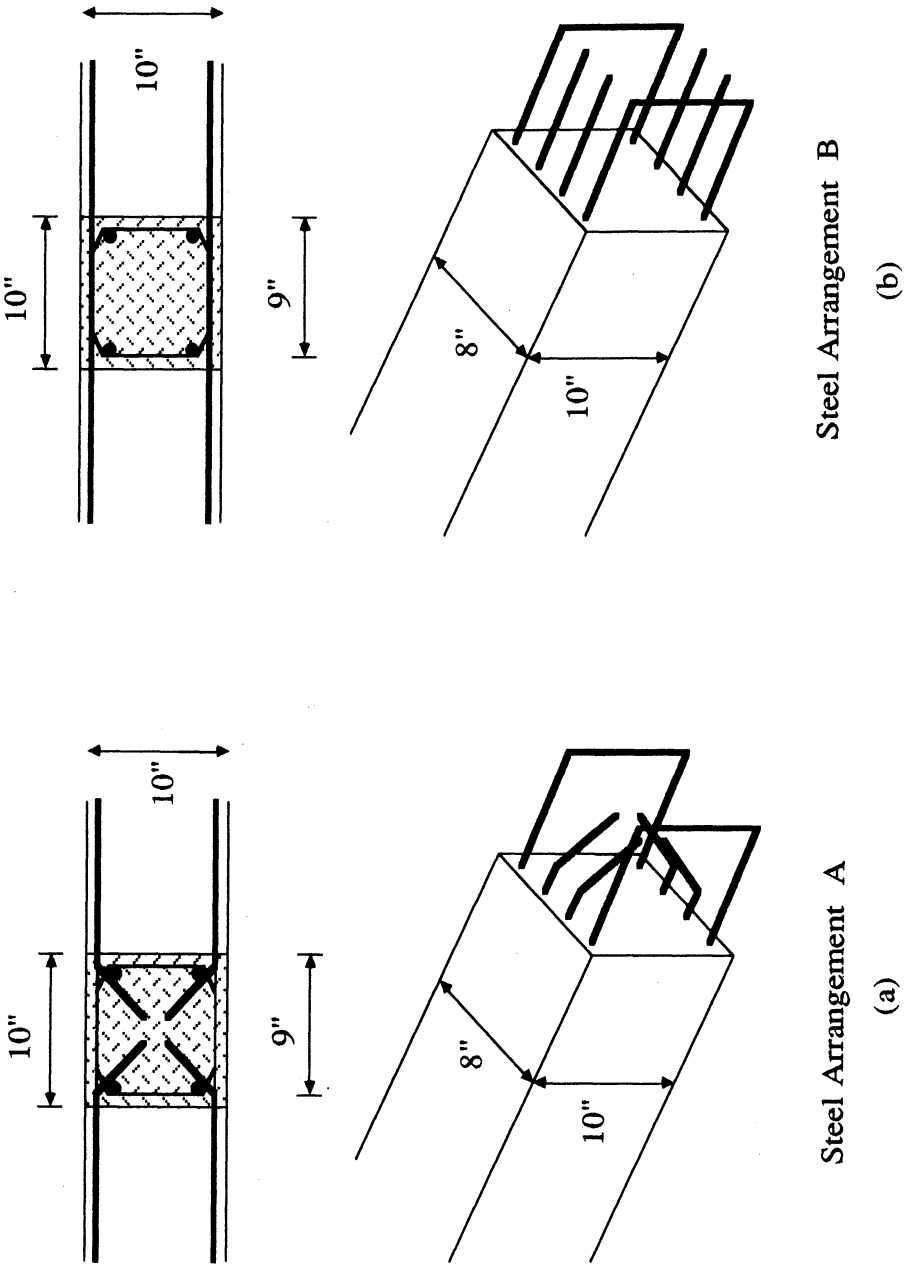

Fig. 3.1- Steel configurations inside the CIP joint for different specimens.

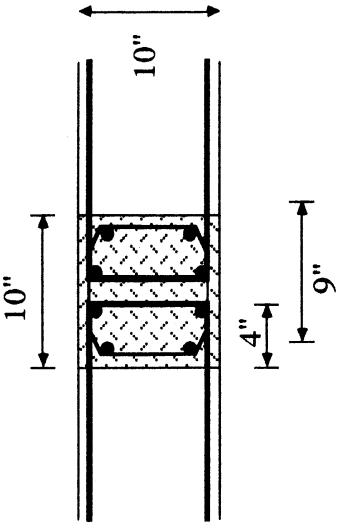

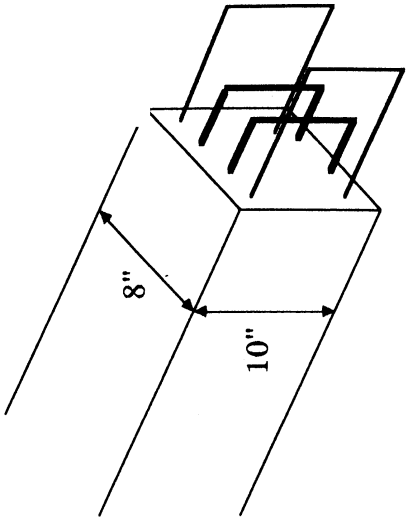

Steel Arrangement D

(d)

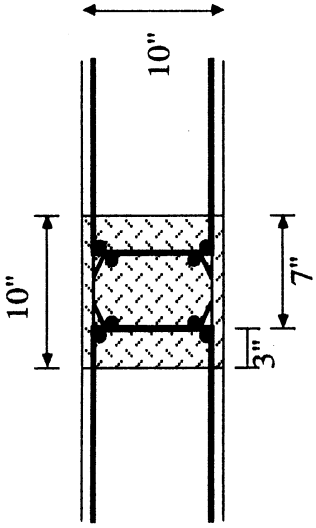

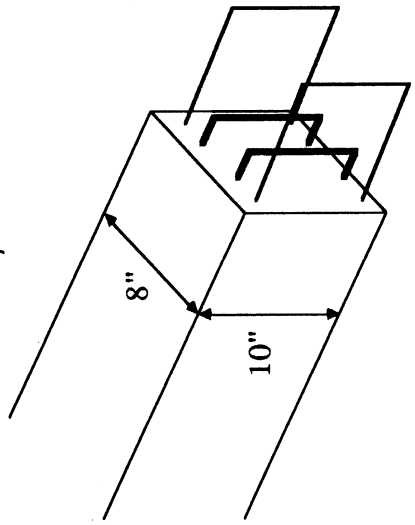

Steel Arrangement C

(c)

Fig. 3.1 (cont'd)

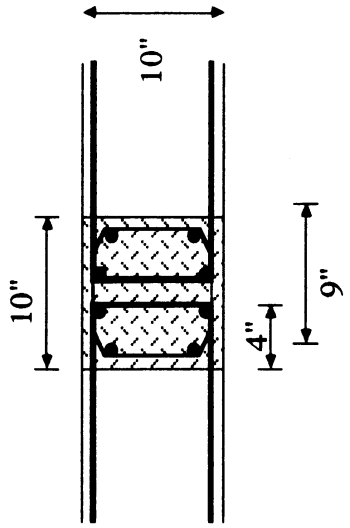

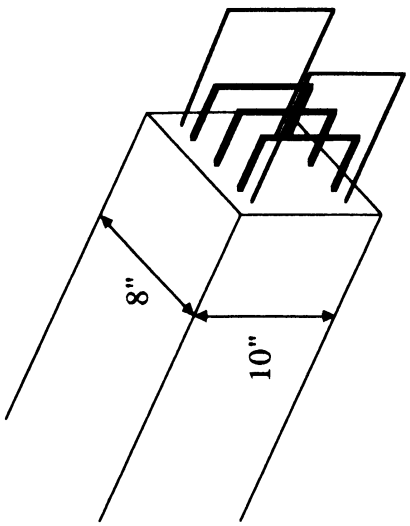

Steel Arrangement D'

(f)

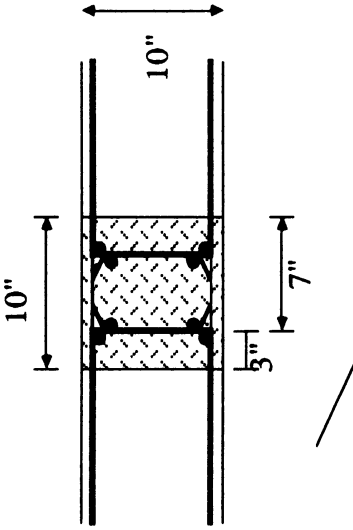

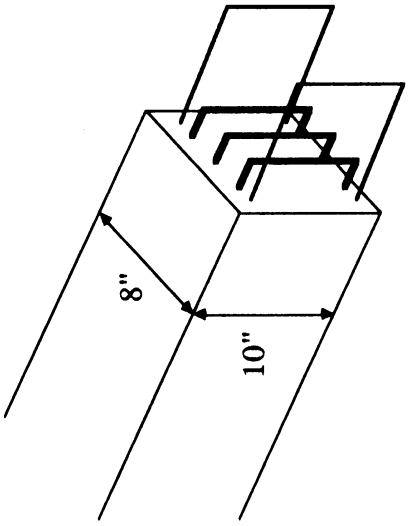

Steel Arrangement C'

(e)

Fig. 3.1 (cont'd)

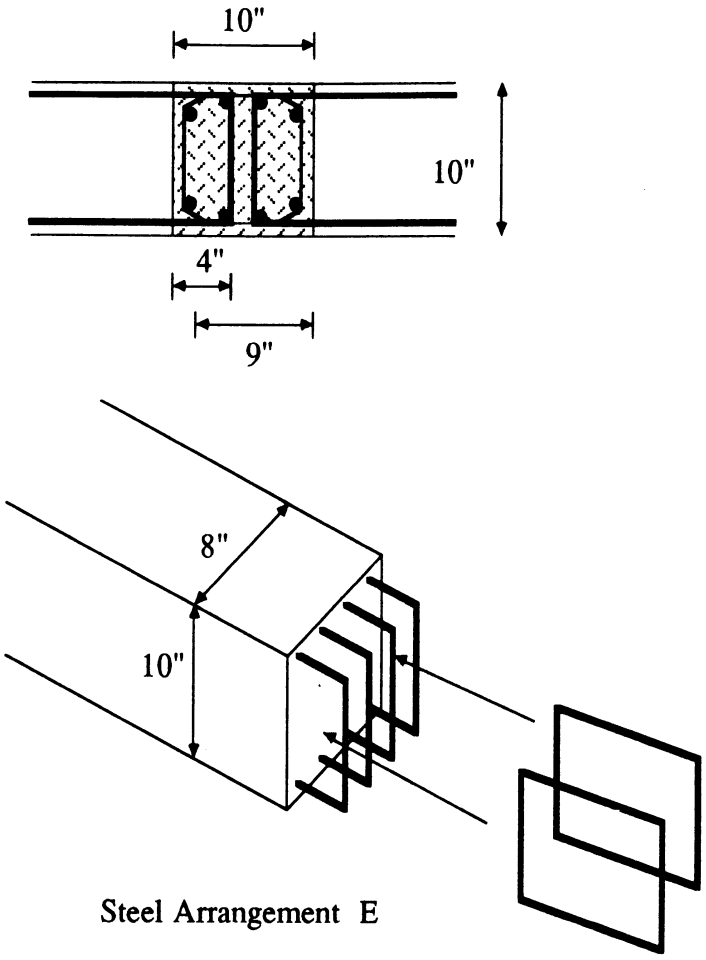

Steel Arrangement E

(g)

Fig. 3.1 (cont'd)

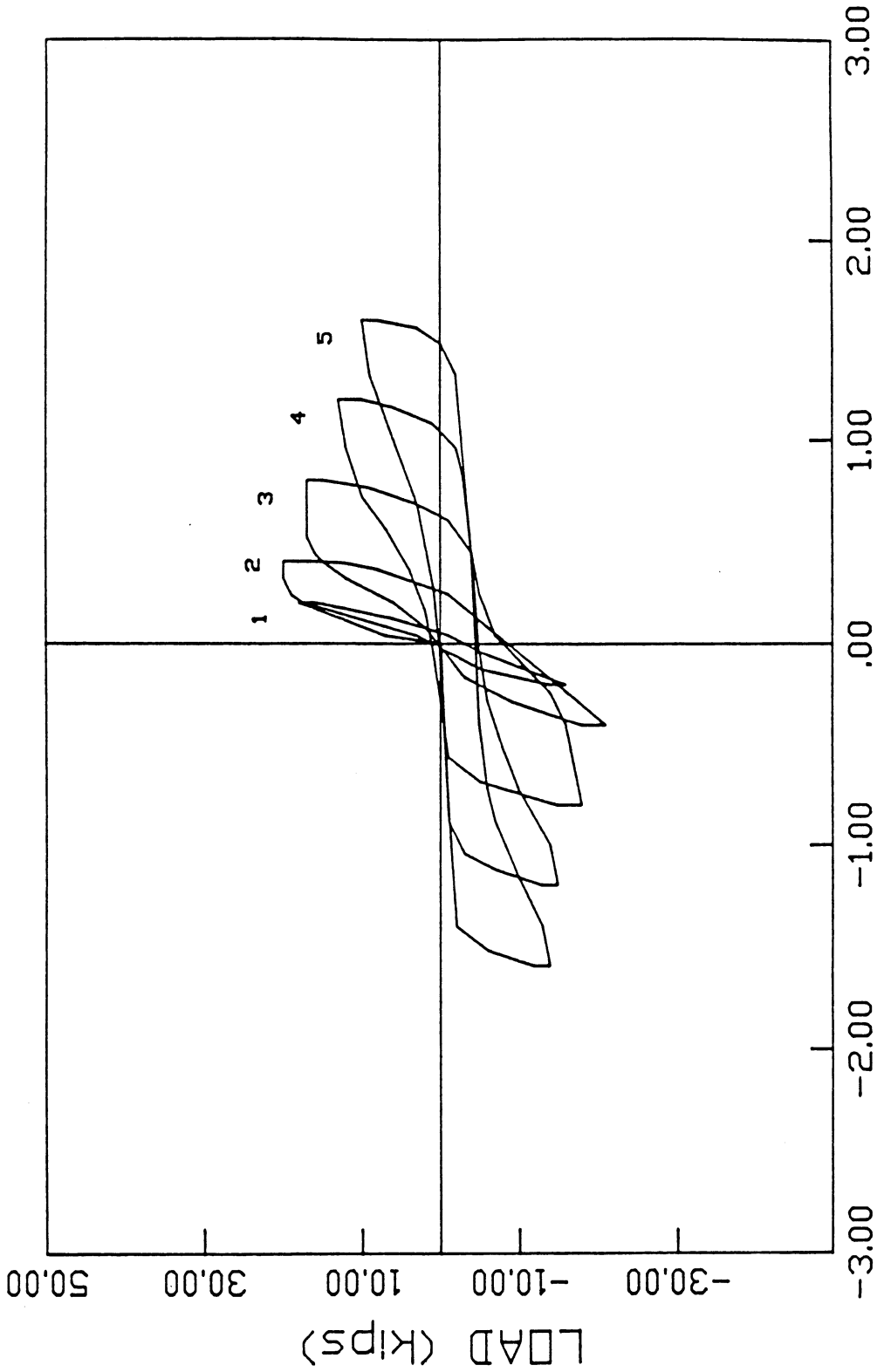

Fig. 3.2 (a)- Load vs. Deflection hysteresis curve for specimen B1.

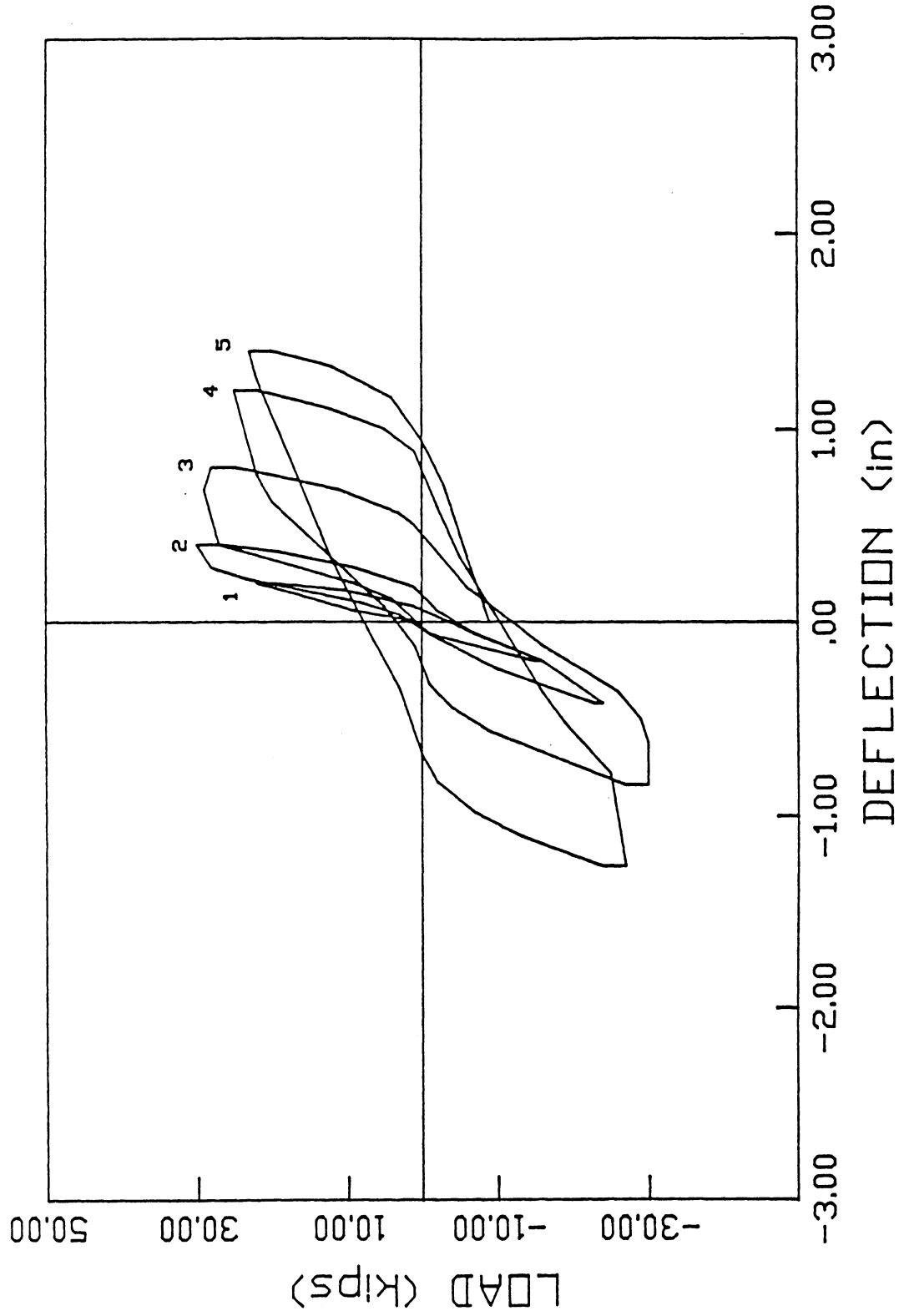

Fig. 3.2 (b)- Load vs. Deflection hysteresis curve for specimen B2.

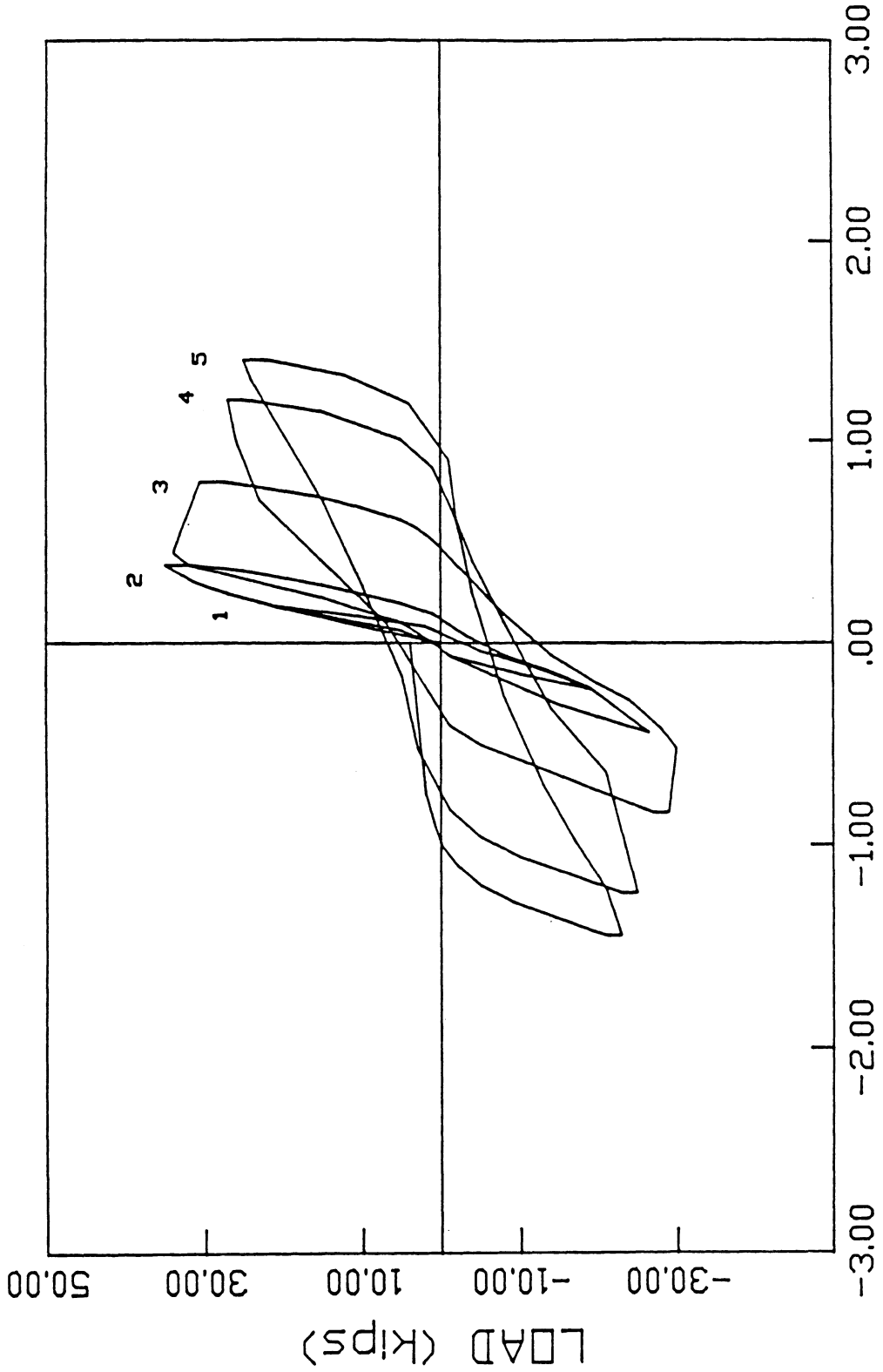

Fig. 3.2 (c)- Load vs. Deflection hysteresis curve for specimen B3.

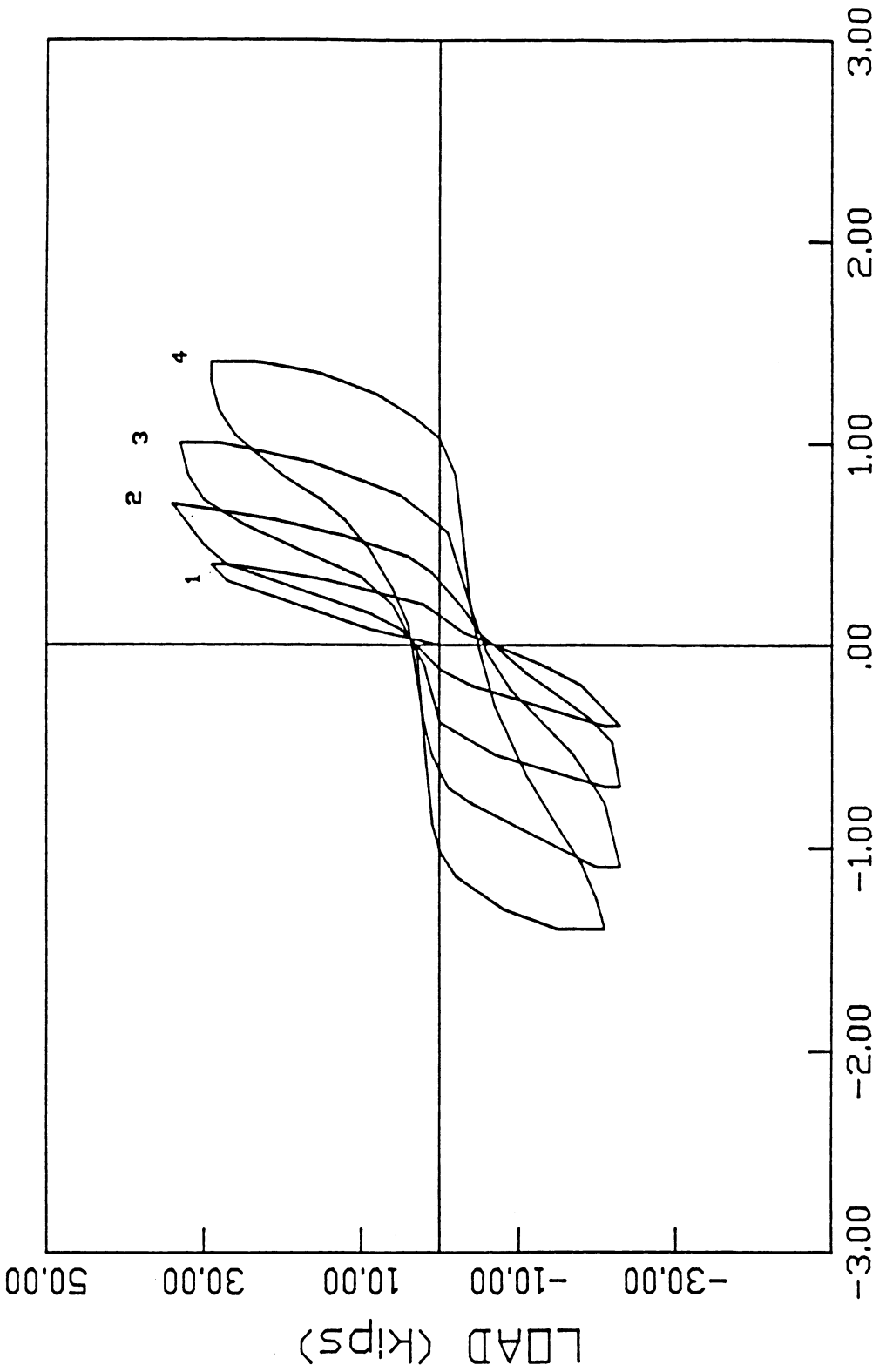

Fig. 3.2 (d)- Load vs. Deflection hysteresis curve for specimen B4.

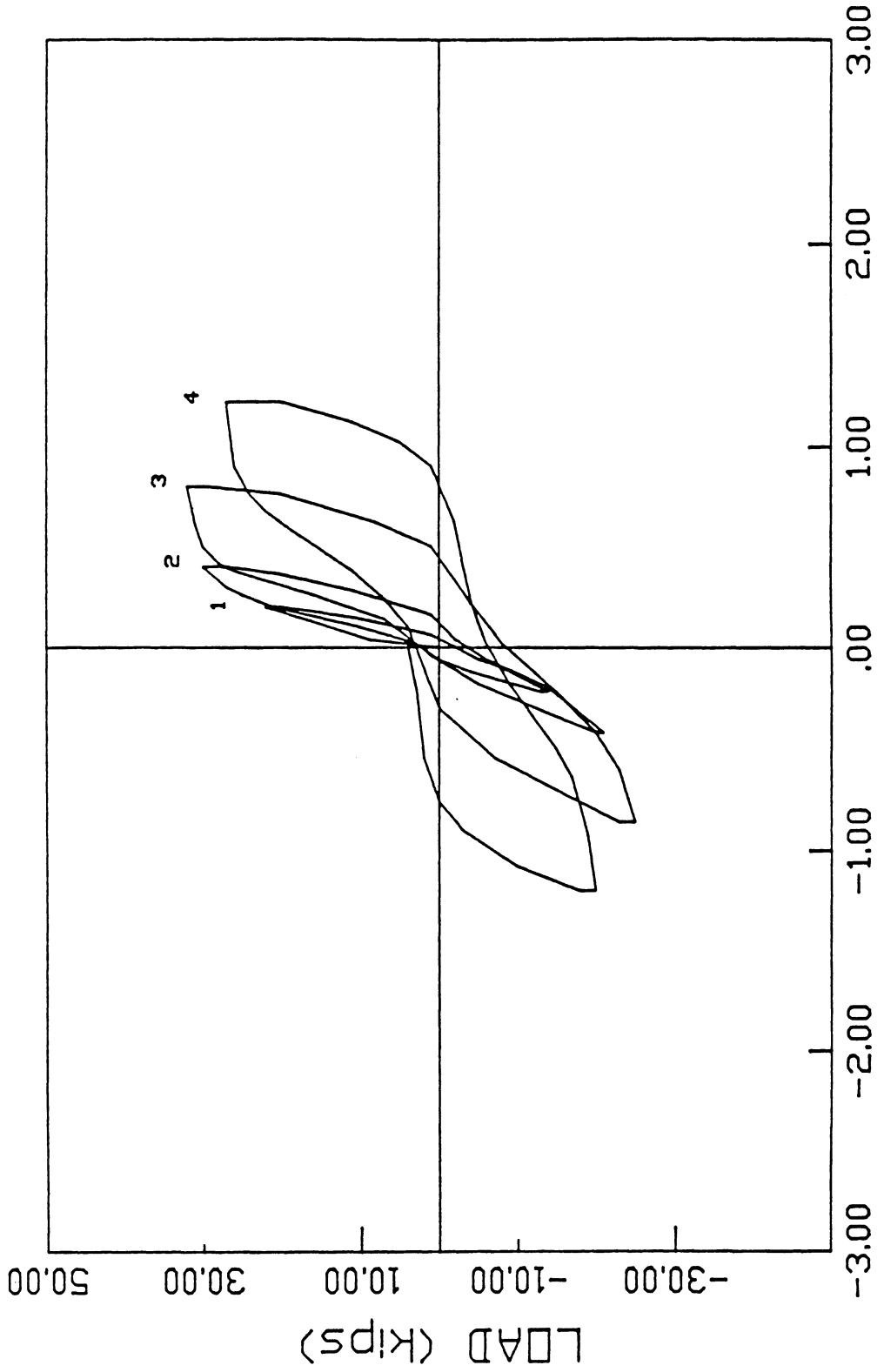

Fig. 3.2 (e)- Load vs. Deflection hysteresis curve for specimen B5.

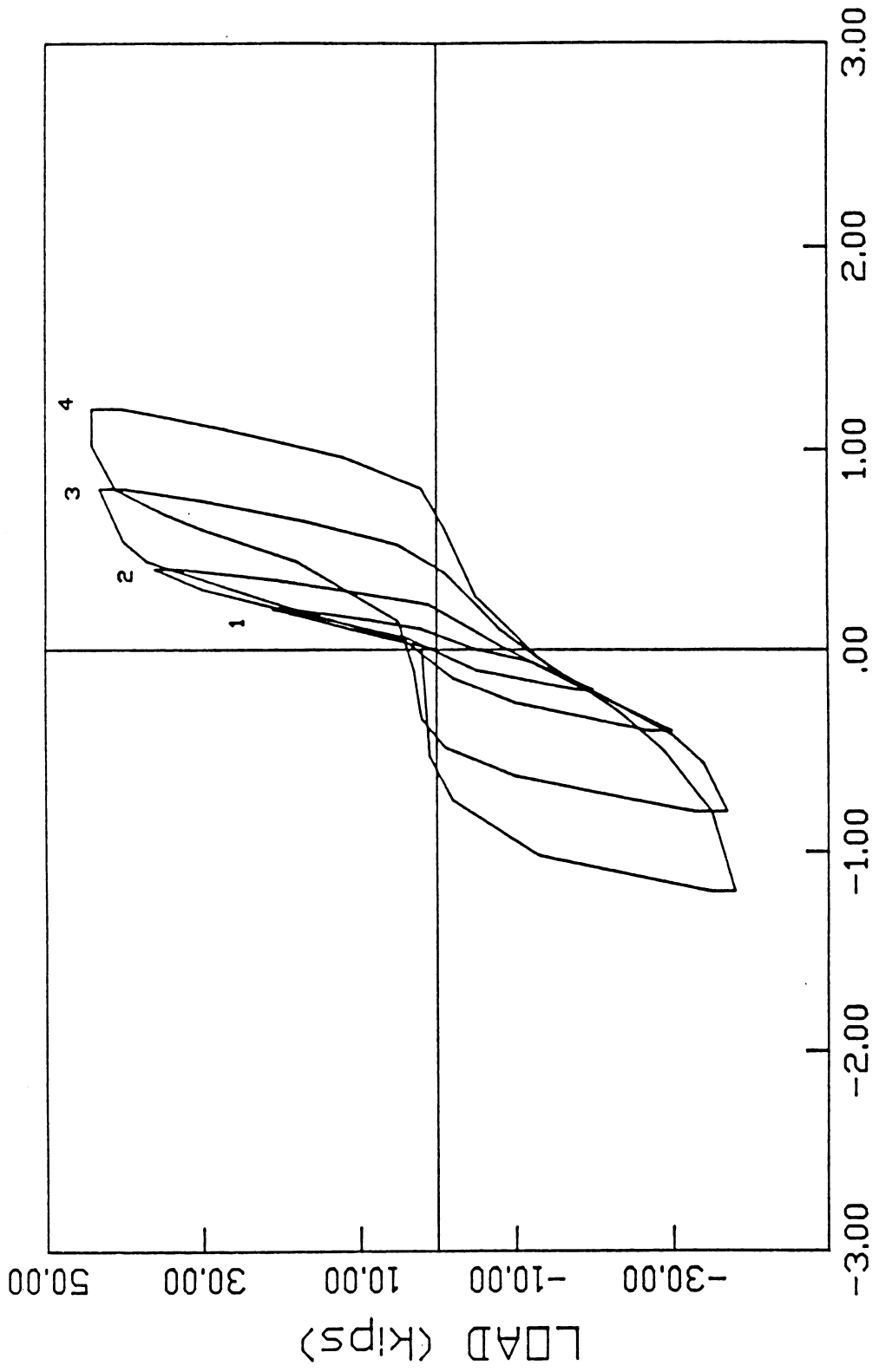

Fig. 3.2 (f)- Load vs. Deflection hysteresis curve for specimen B6.

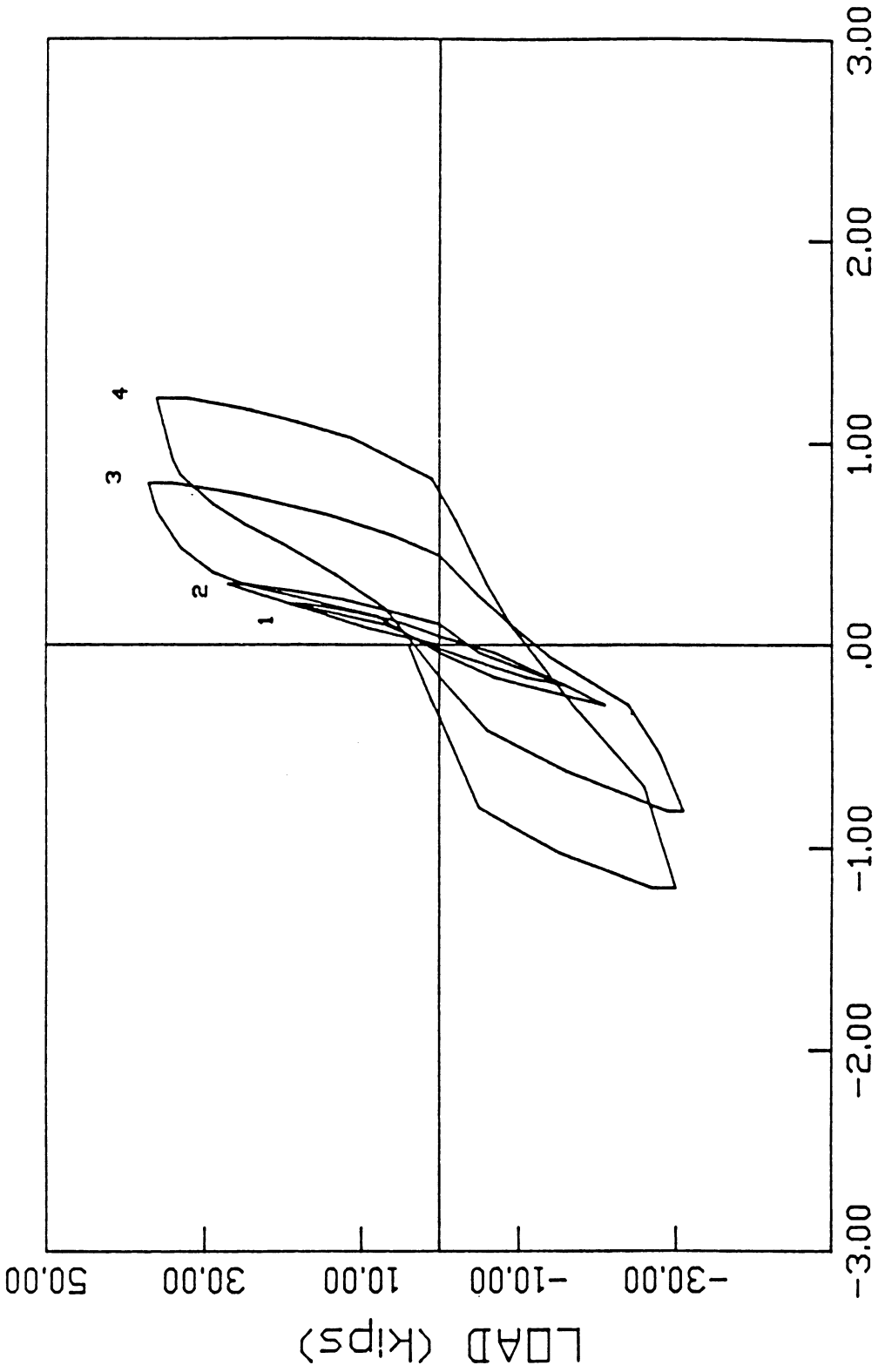

Fig. 3.2 (g)- Load vs. Deflection hysteresis curve for specimen B7.

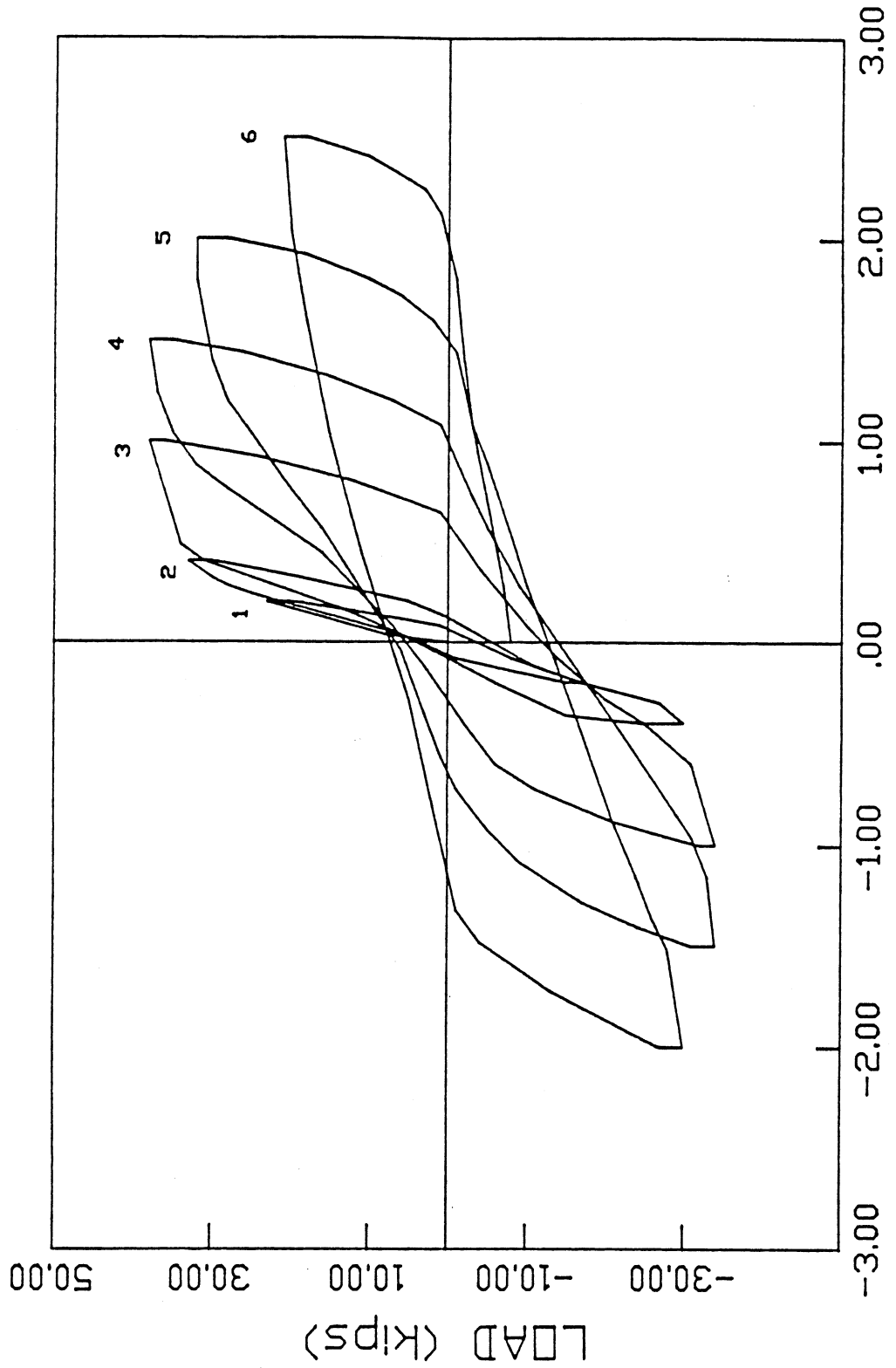

Fig. 3.2 (h)- Load vs. Deflection hysteresis curve for specimen B8.

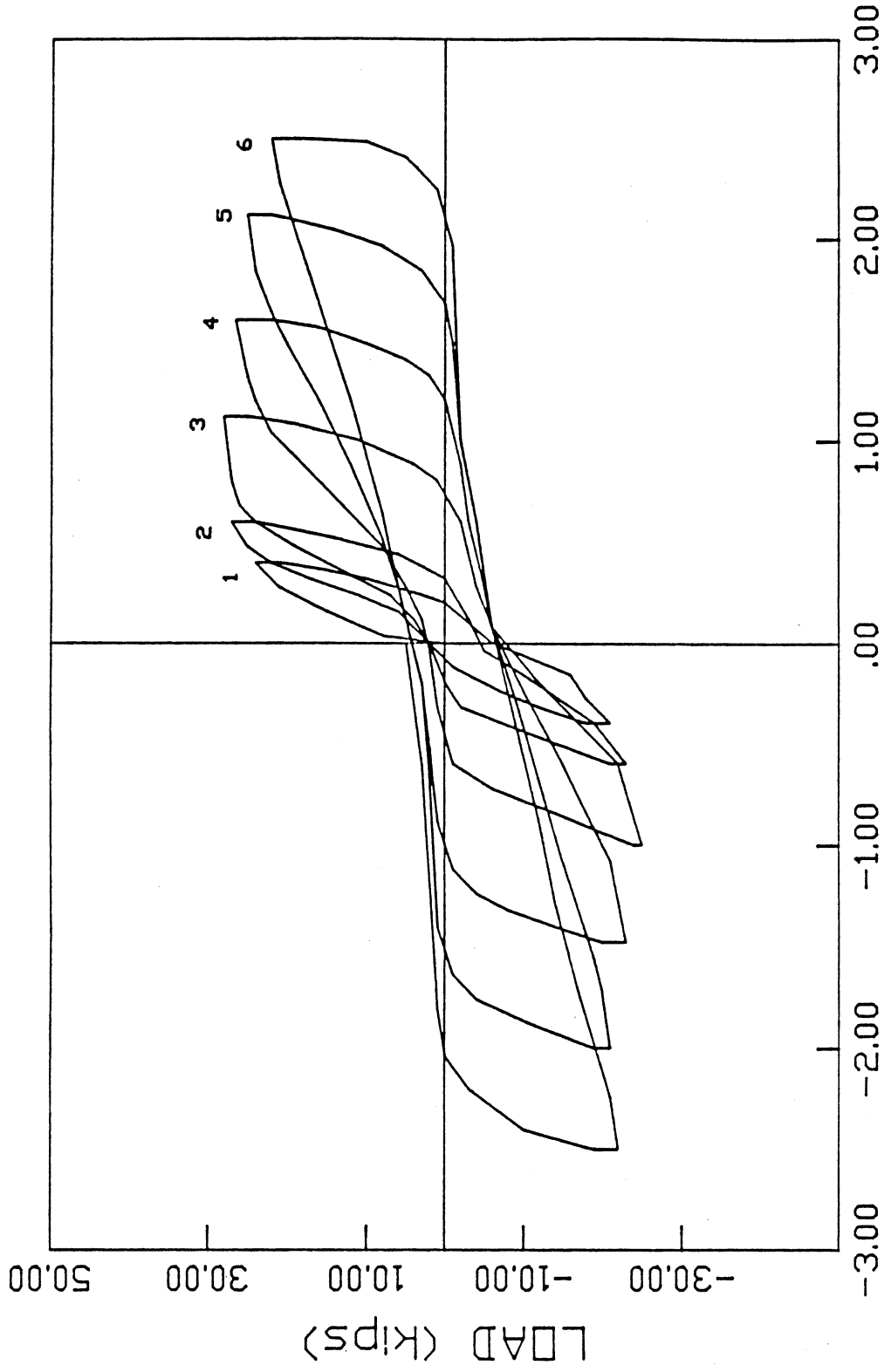

Fig. 3.2 (i)- Load vs. Deflection hysteresis curve for specimen B9.

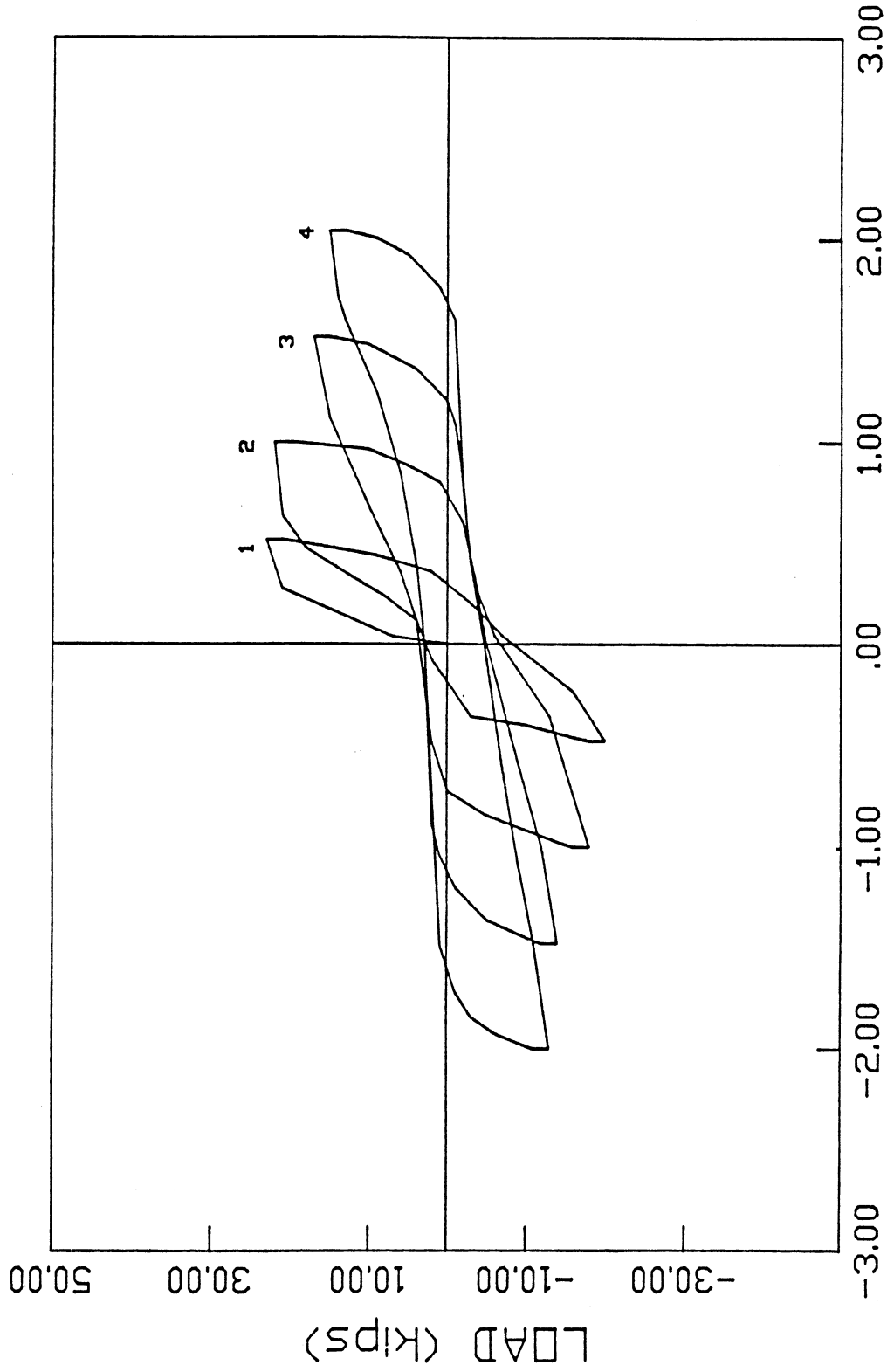

Fig. 3.2 (k)- Load vs. Deflection hysteresis curve for specimen B11.

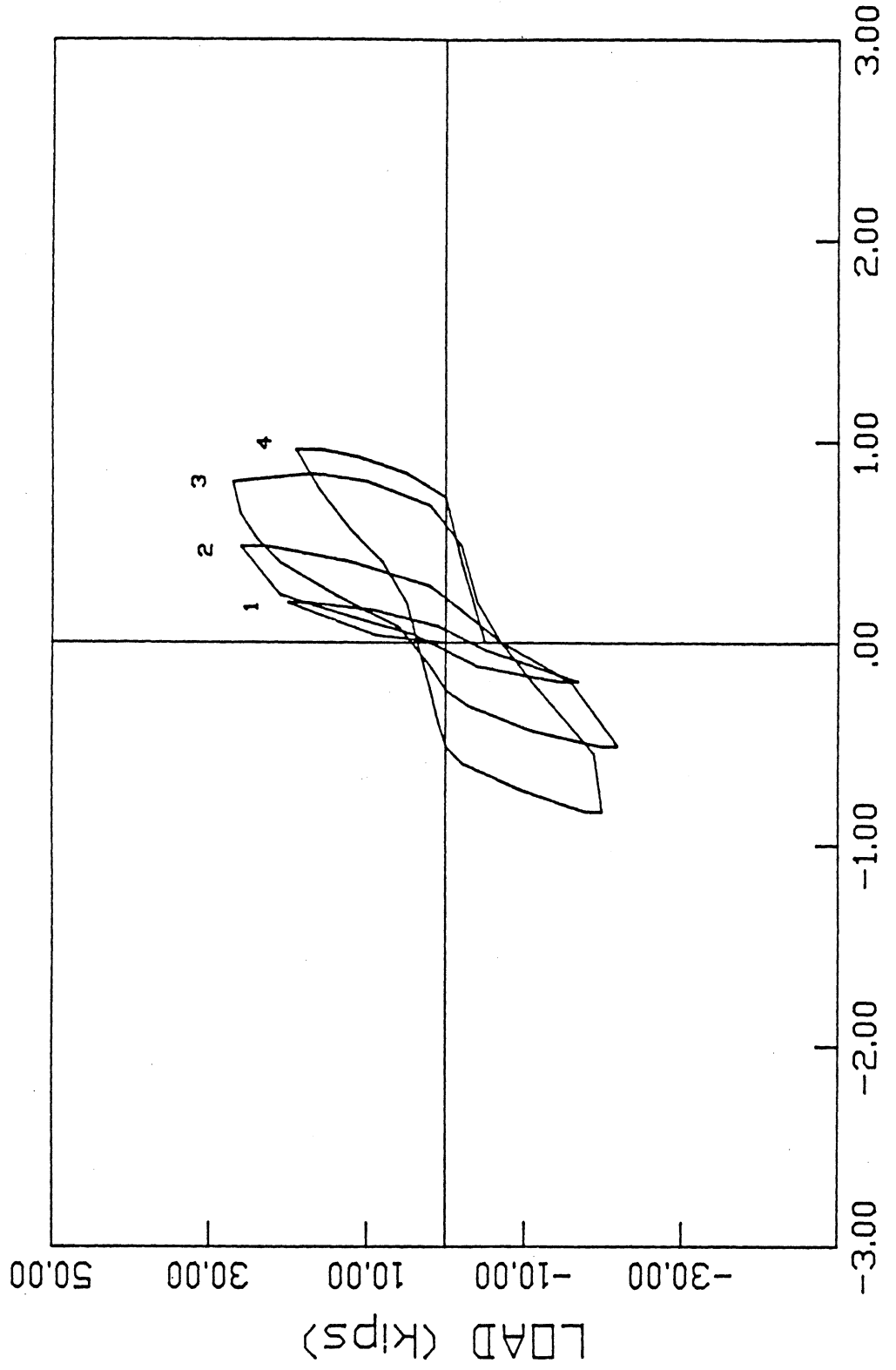

Fig. 3.2 (l)- Load vs. Deflection hysteresis curve for specimen B12.

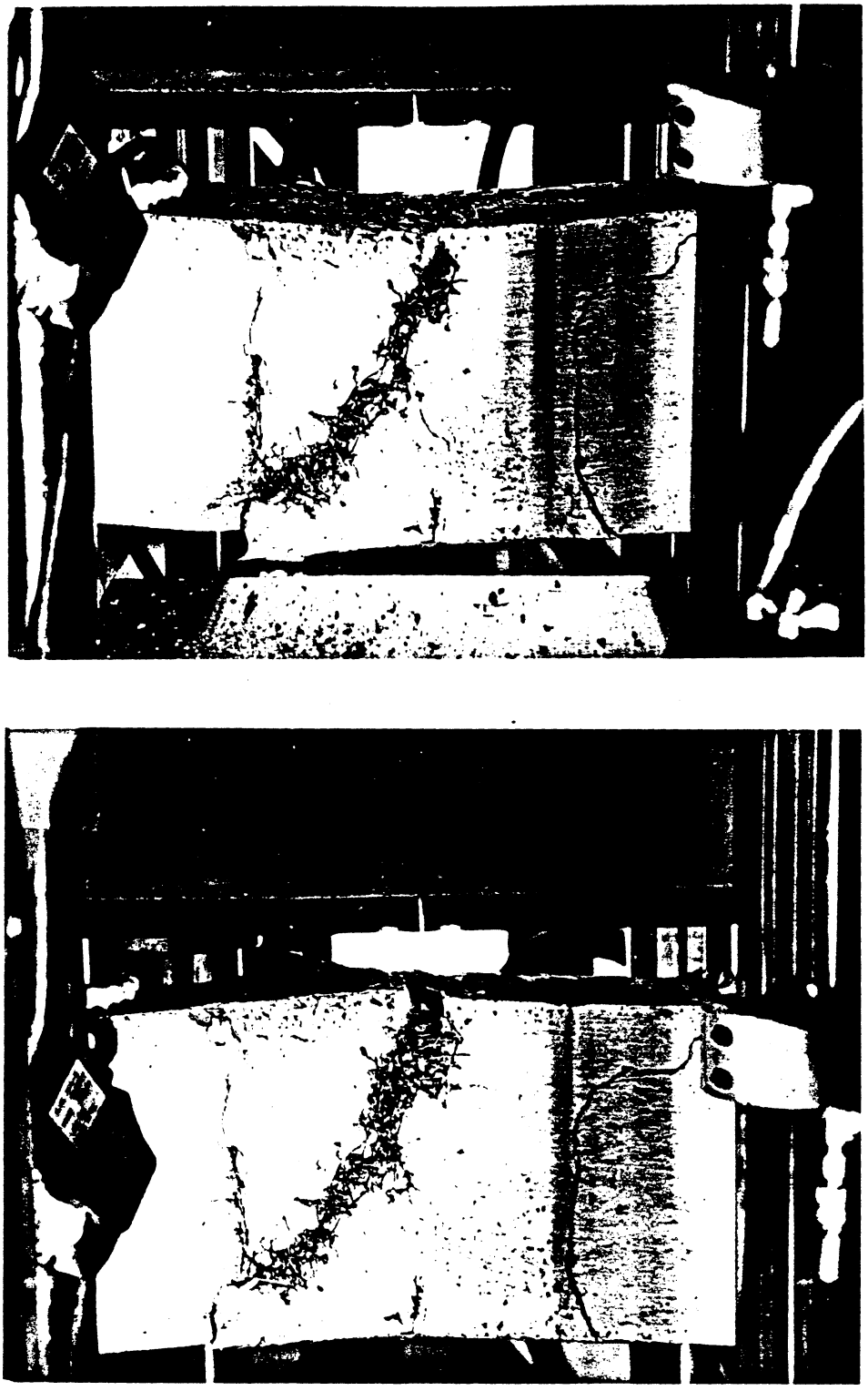

Fig. 3.3 (a)- Specimen B1 at the end of the test in the upward and downward directions.

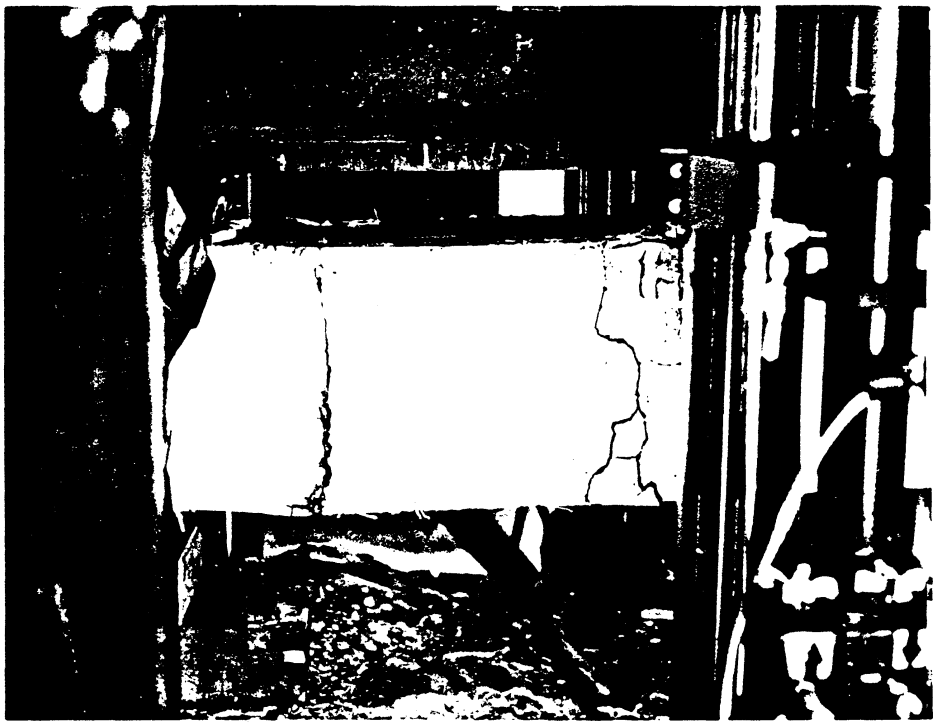

Fig. 3.3 (b)- Specimen B2 at the end of the test.

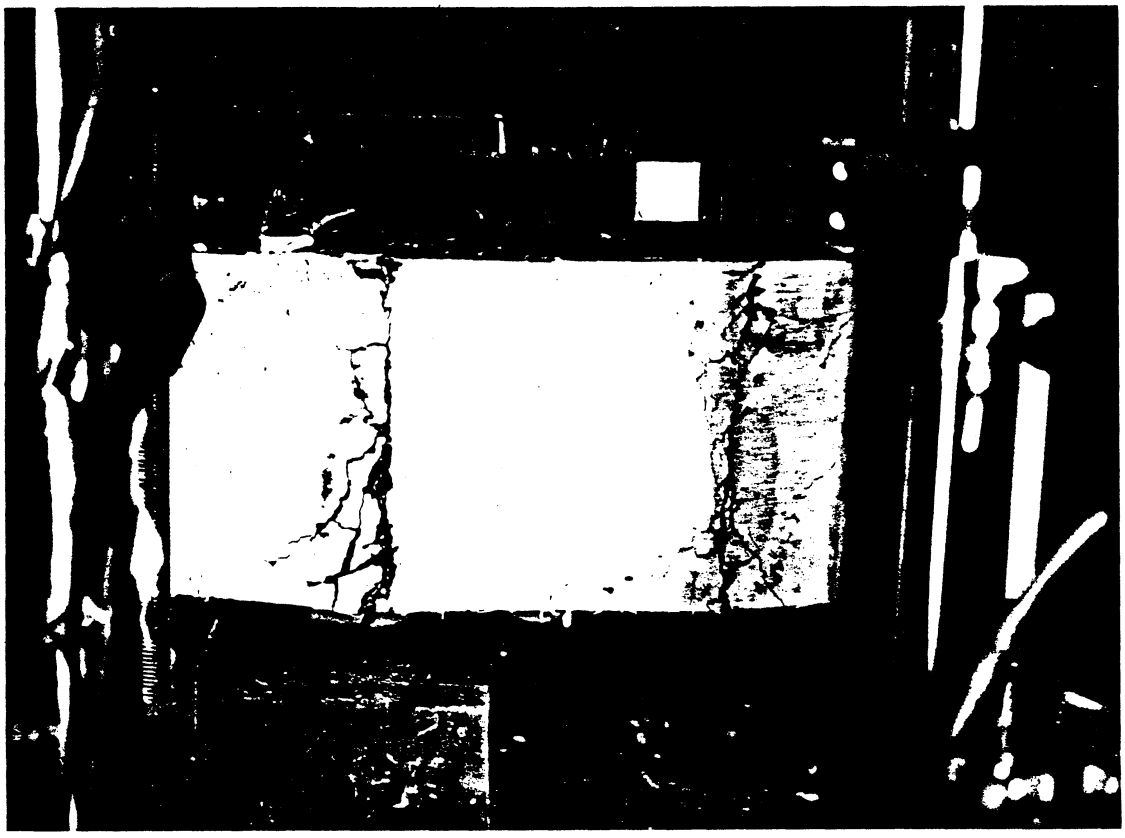

Fig. 3.3 (c)- Specimen B3 at failure.

Fig. 3.3 (d)- Specimen B4 at the end of the test.

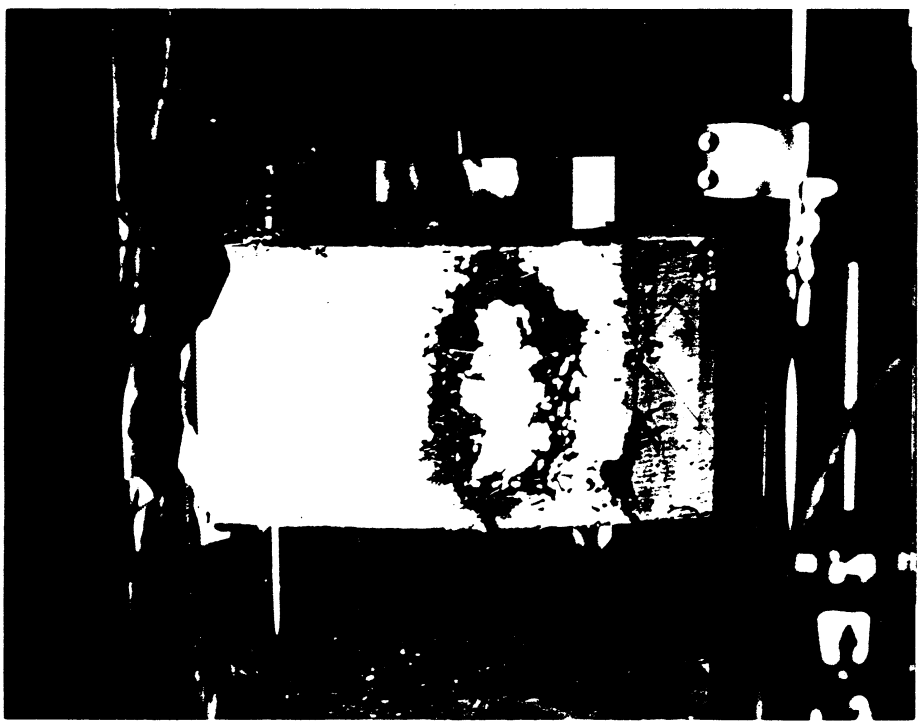

Fig. 3.3 (e)- Specimen B5 at failure.

Fig. 3.3 (f)- Specimen B6 at the end of the test.

Fig. 3.3 (g)- Specimen B7 at failure.

Fig. 3.3 (h)- Specimen B8 at the end of the test.

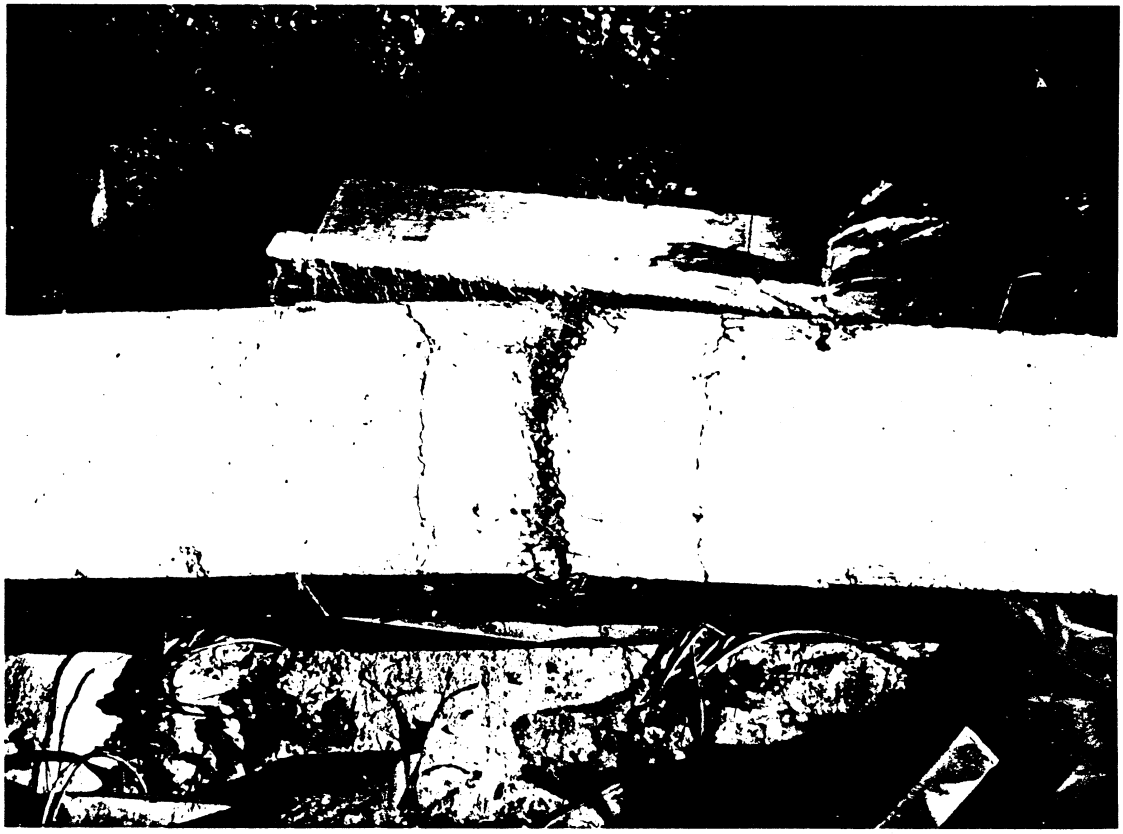

Fig. 3.3 (i)- Specimen B9 at failure.

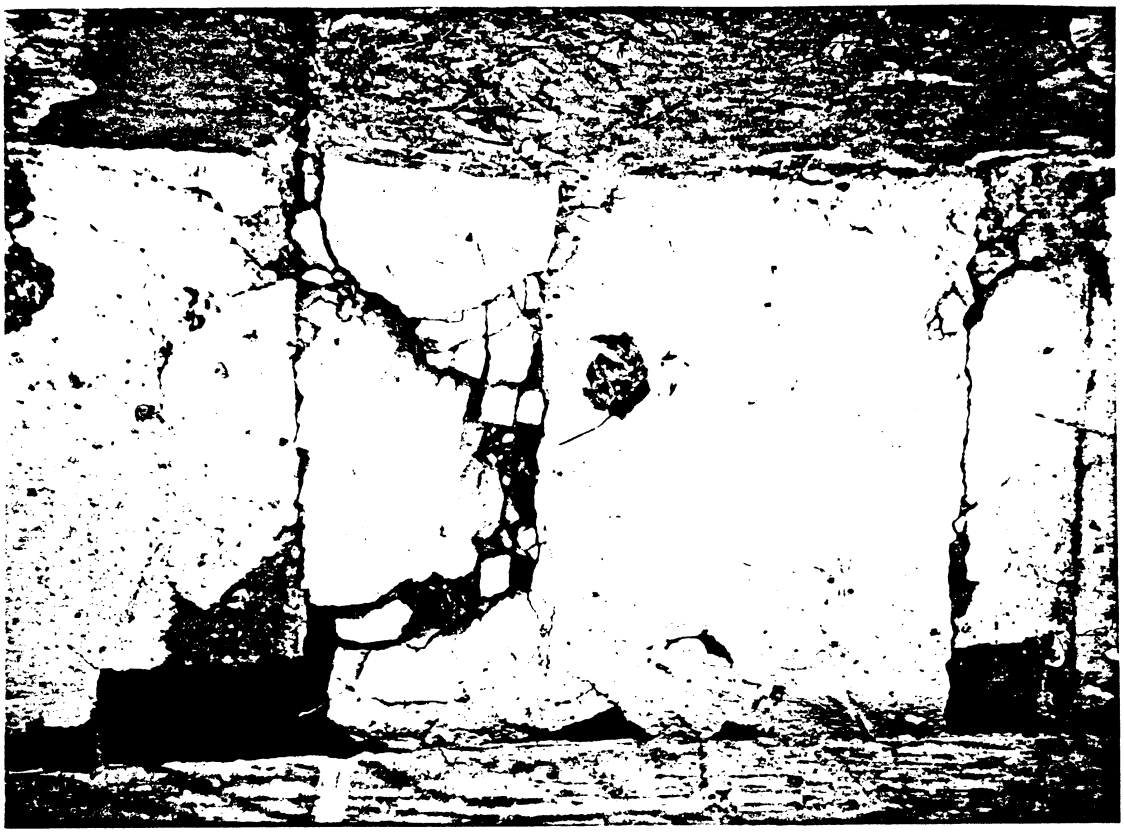

Fig. 3.3 (j)- Specimen B10 at the end of the test.

Fig. 3.3 (k)- Specimen B11 at failure.

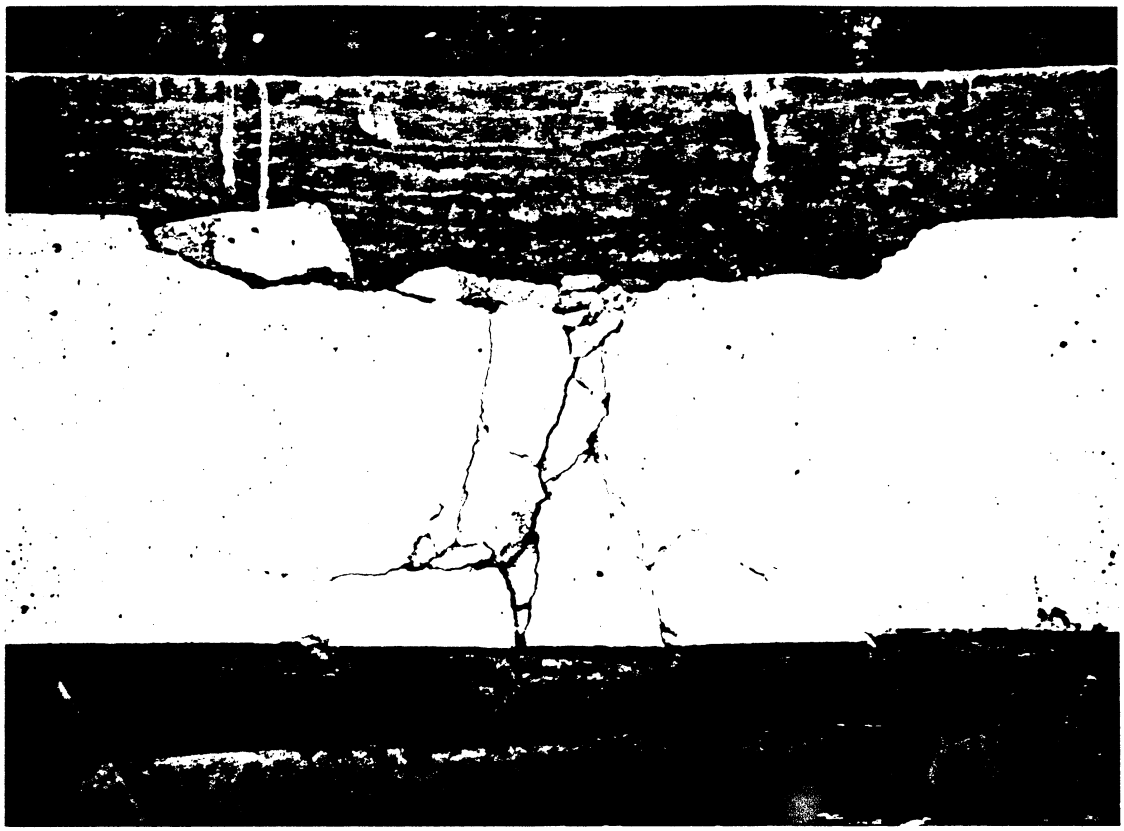

Fig. 3.3 (l)- Specimen B12 at failure.